The Importance of Heterogeneity in Dynamic Network Models Applied to European Systemic Risk*

Xingmin Zhang[a], Anne Opschoor[b], and André Lucas[b]

January 28, 2022

[a] *School of Finance, Southwestern University of Finance and Economics*
[b] *Vrije Universiteit Amsterdam and Tinbergen Institute*

Abstract

Standard spatial time-series models for financial networks can fail substantially in uncovering empirical network and risk dynamics. We propose a novel empirical spatial modeling framework that solves this problem by accommodating both heterogeneity and time-variation in economic connections and spillovers. While highly flexible, the model is still straightforward to estimate. We apply the model to several datasets for Eurozone sovereign credit risk during the sovereign debt crisis. Accounting for heterogeneity and time-variation turns out to be empirically important and the new model uncovers intuitive patterns that would go unnoticed otherwise in currently available homogeneous and/or static spatial financial network models.

Keywords: dynamic networks, spatial auto-regressions, heterogeneous spatial contagion, network heterogeneity, sovereign risk dynamics.

1 Introduction

Spatial models have a long history in economics and regional science. More recently, however, spatial models have also attracted quite some attention in financial economics to describe networks

*We thank Bernd Schwaab and seminar participants at Vrije Universiteit Amsterdam for suggestions that helped to improve the paper. This research was initiated when Zhang was visiting Vrije Universiteit Amsterdam on a Chinese Research Council scholarship. Zhang acknowledges financial support from National Natural Science Foundation of China (No.72101209).

of firms and markets. Starting with the spatial models of Fernandez (2011), Fernández-Avilés et al. (2012) and Asgharian et al. (2013) to study international stock market linkages, spatial models have been used across a wide variety of areas, including studies into asset pricing implications of network connections (Kou et al., 2018), cross-sectional market volatility patterns as related to firm connections (Herskovic et al., 2020), financial markets and banking sector stability (Tonzer, 2015; Milcheva and Zhu, 2016; Pino and Sharma, 2019), contagion across energy markets (Demirer et al., 2020) and credit ratings (Asgharian et al., 2013), and pricing and portfolio implications in real estate markets (Zhu and Lizieri, 2021; Zhu and Milcheva, 2020). Also from a theoretical perspective, spatial models for networks naturally emerge as Nash equilibria as in for instance Denbee et al. (2021).

In all these models, the strengths of the linkages between network players is typically captured by a matrix of observable variables, which may vary over time. For instance, in our application we use quarterly cross-border banking claims in the Eurozone to measure spatial weights; see also Tonzer (2015) and Blasques et al. (2016). On top of the relative connection strengths in the network as captured by the observables, the overall strength of all connections in the network is generally captured by a single, static parameter. This imposes quite some restrictions on the model specification. In dynamic and stressed settings such as a crisis, different players in the network might have a sensitivity to other players in the network that increases or decreases disproportionately during such periods. Such movements may not be captured by the observables used to describe the approximate network connections. This poses two main challenges to most of the spatial models used thus far to describe financial networks.

First, as indicated by Aquaro et al. (2021), there is a need to allow for more heterogeneity in the spatial model parameters that describe the sensitivities of different players to shocks elsewhere in the network. They show that standard scalar spatial models are typically inadequate and may obscure and bias important patterns in the data. More heterogeneity in the spillover parameters is called for to capture the network structure well. This finding is also in line with Herskovic et al. (2020), who allow for different network sensitivities of firms in a set-up where connections between firms are measured. Both Aquaro et al. (2021) and Herskovic et al. (2020) use heterogeneous, but static extensions of the baseline spatial model for financial networks. This brings us to the second challenge: time-variation in the network connections. Blasques et al. (2016), Catania and Billé (2017), and Billé et al. (2019) show that the overall strength of network connections can change substantially over time in stock markets, debt markets, and real estate markets. These papers introduce dynamic extensions of the baseline spatial model that allow for additional dynamics in network propagation strength on top of what is captured by simple observable variables. All three papers do so with one (possibly two) dynamic parameters. The results allow one to obtain

additional measures of systemic stress and network fragility that exhibit more dynamics during turbulent times compared to the typical static models available in the current literature. Still, these models allow for only a limited amount of (dynamic) heterogeneity across the network players; compare Aquaro et al. (2021). This may severely bias the results against time-variation in network propagation strength and hide important features of the network and its dynamics. For example, Blasques et al. (2016) find evidence of time-varying spillover strength for European sovereign debt, but the time-variation is surprisingly modest given the variety of countries included in their analysis. This is likely to be due to over-restrictive pooling assumptions in the model specification.

This paper develops a new spatial dependence model for dynamic networks with heterogeneous spatial spillover parameters, thus filling an important gap in the empirical finance literature for dynamic network modeling. On top of time-variation in network connections via observed variables, we introduce separate time-varying spatial dependence parameters such that each network player can have its own time-varying sensitivity to what happens elsewhere in the network. Empirically and in simulations, we find that allowing for both heterogeneity and time-variation are important. If the dynamics are omitted, differences in fragility of the network over time are not captured adequately. Conversely, if heterogeneity is omitted, a scalar dynamic spatial parameter only provides a very blurred picture of the different positions of the network players over time. For instance, if the network importance of some countries plays up over time, whereas that of others wanes, the overall scalar summary measure might incorrectly signal nothing is happening in the network at all. Again, this may lead to flawed inference and an incorrect assessment of the true underlying economic mechanisms. The new model avoids these issues and allows us to capture both the heterogeneity, dynamics, and asymmetric risk propagation between network members much more accurately. Despite all this added flexibility, the new model is still straightforward to estimate.

To illustrate the importance of both heterogeneity and time-variation in financial and economic networks, we apply our model to three different datasets related to European sovereign credit risk. Our baseline analysis uses weekly changes in 5 year government bond spreads over the OIS EONIA rate for 7 European countries over the period 2009-2020. We find that allowing for heterogeneous dependence parameters improves the statistical fit compared to the scalar spatial model of Blasques et al. (2016), as well as compared to static heterogeneous models or static scalar models, like the original model of Anselin (2009). Important features characterizing the dynamics of the European sovereign debt crisis become clear in the new heterogeneous dynamic model. This includes the anchoring role of Germany as well as the risk sensitivities of countries like Spain, Portugal, Ireland, and particularly Italy. Allowing for heterogeneous, time-varying spatial dependence parameters leads to an increase in both the short- and long-run spillover risk, in some cases by factors more

than five. Again, we stress that all such features would go unnoticed in homogeneous or static versions of the model such that it is empirically important to allow for both heterogeneity and time-variation in financial networks.

Our study contributes to several lines of literature. On the one hand, it opens an new avenue to investigate financial network properties in a much more flexible way than with the static models used in for instance Asgharian et al. (2013), Kou et al. (2018), Herskovic et al. (2020), and other references mentioned earlier. Given the empirical relevance of both heterogeneity and time-variation, it may also call for further theoretical advances of baseline frameworks such as in Denbee et al. (2021) to explain such time-variation. Our paper also links to the extant literature on modeling financial networks to study risk propagation and financial stability, such as for instance Acharya et al. (2014), Williamson (2003), Elliott et al. (2014), and Fernandes and Artes (2016). Recent literature on systemic risk highlights the importance of spatial dependence and network spillovers (e.g., Asgharian et al., 2013; Babii et al., 2019). Finally, methodologically our work relates to the literature on score-driven time-varying parameter models as in Creal et al. (2013). A similar score-driven approach is found in Blasques et al. (2016), Catania and Billé (2017), and Billé et al. (2019). As mentioned before, however, our work differs from theirs in that we allow for more dynamic heterogeneity across network players, which proves empirically highly important. As such, our new spatial specification could also be used to measure contagion effects and systemic risk; see Franklin and Douglas (2000); Billio et al. (2012); Acemoglu et al. (2015). We are also aware of a parallel line of literature that measures network effects via vector autoregressive models and a variance decomposition; see Diebold and Yılmaz (2014). In contrast to this approach, the spatial approach extended in this paper provides directed links rather than symmetric links only. Our work thus mainly concentrates on providing a way forward compared to the static and homogeneous spatial models that are used in many contemporary analyses of financial and economic networks; see for instance Kou et al. (2018), Herskovic et al. (2020), or Tonzer (2015).

The remainder of this paper is organized as follows. Section 2 discusses the new model. The data are discussed in Section 3, followed by the empirical results in Section 4. Section 5 presents robustness checks. Section 6 concludes.

2 Empirical model

2.1 Spatial autoregressions

Rather then building up the model step-by-step, we provide the most general form of the model first and then highlight how earlier models are special cases of this more general specification. We

gather the relevant measurements of a network into the vector $\boldsymbol{y}_t$. For instance, in our setting $\boldsymbol{y}_t$ contains spread changes of sovereigns in the Eurozone, but the measurements might just as well relate to stock returns in a network of connected firms. We use the following vector-valued time-varying parameter spatial autoregressive (SAR) model for $\boldsymbol{y}_t$,

$$\boldsymbol{y}_t = \boldsymbol{R}_t \boldsymbol{W}_t \boldsymbol{y}_t + \boldsymbol{X}_t \boldsymbol{\beta} + \boldsymbol{\varepsilon}_t, \qquad \boldsymbol{\varepsilon}_t \overset{iid}{\sim} p_{\boldsymbol{\varepsilon}}(\boldsymbol{\varepsilon}_t; \boldsymbol{\Sigma}_t, \nu), \tag{1}$$

where $\boldsymbol{y}_t = (y_{1,t}, \ldots, y_{N,t})^\top \in \mathbb{R}^{N \times 1}$ denotes the vector of cross sectional measurements for time $t = 1, \ldots, T$, where the cross-section dimension i relates to the network players, $\boldsymbol{\varepsilon}_t \in \mathbb{R}^{N \times 1}$ is a serially independently and identically distributed error term or vector of 'structural' shocks with a density $p_{\boldsymbol{\varepsilon}}(\boldsymbol{\varepsilon}_t; \boldsymbol{\Sigma}_t, \nu)$ such as the normal distribution or alternatively a fat-tailed Student's t distribution. The density is characterized by a diagonal covariance matrix $\boldsymbol{\Sigma}_t$ and a static parameter ν. Furthermore, $\boldsymbol{X}_t \in \mathbb{R}^{N \times K}$ denotes a matrix holding exogenous regressors with corresponding static parameter vector $\boldsymbol{\beta} \in \mathbb{R}^{K \times 1}$, $\boldsymbol{W}_t \in \mathbb{R}^{N \times N}$ is an observable matrix containing the spatial weights, and $\boldsymbol{R}_t \in \mathbb{R}^{N \times N}$ is a diagonal matrix containing the unobserved time-varying heterogeneous spatial spillover parameters, also called spatial autoregressive coefficients. The spatial spillover parameters in $\boldsymbol{R}_t$ play a major role in the subsequent analysis. The model in (1) is already dynamic via the observed $\boldsymbol{W}_t$ matrix that measures the time-varying connections in the network in the standard way. On top of this, (1) also allows for further unobserved heterogeneity via the matrix $\boldsymbol{R}_t$. More on this follows below.

The model in (1) nests several models from the literature. For example, if $\boldsymbol{\Sigma}_t = \boldsymbol{\Sigma}$ and $\boldsymbol{R}_t \equiv \rho \cdot \mathbf{I}_N$ for a scalar ρ with $\mathbf{I}_N \in \mathbb{R}^{N \times N}$ the identity matrix, then (1) collapses to the standard spatial regression model; see for instance Anselin (2009), Asgharian et al. (2013), Kou et al. (2018), Denbee et al. (2021). For a static $\boldsymbol{R}_t = \boldsymbol{R}$, we obtain the model with static heterogeneous spillover strengths as in Aquaro et al. (2021) and Herskovic et al. (2020). The static model $\boldsymbol{R}_t = \rho \cdot \mathbf{I}_N$ was generalized to a setting with a time-varying spatial autoregressive parameter ρ_t by Blasques et al. (2016) and Catania and Billé (2017). We also obtain this scalar dynamic model as a special case by setting $\boldsymbol{R}_t = \rho_t \cdot \mathbf{I}_N$. However, our new model that allows $\boldsymbol{R}_t$ to be a non-scalar matrix, provides a much richer description of the spatial dynamics of the model. In particular, some network units may be important contributors to systemic risk at some times, whereas other units may take over this role at other times. This is captured by the different diagonal elements of $\boldsymbol{R}_t$, the ith element measuring the spatial sensitivity of unit i to the other units. Note that (1) also allows the structural shocks to have a time-varying variance $\boldsymbol{\Sigma}_t$. This allows for periods where the flow of information is high compared to other periods. The model can easily be extended further to include, for instance, a spatial lag structure for the error term, or a non-diagonal covariance structure for $\boldsymbol{\varepsilon}_t$.

2.2 Modeling time-variation in spatial dynamics

The time variation in $\boldsymbol{R}_t$ and $\boldsymbol{\Sigma}_t$ can be modeled in different ways. In this paper, we endow $\boldsymbol{R}_t$ and $\boldsymbol{\Sigma}_t$ with score-driven dynamics as proposed in Creal et al. (2011, 2013) and Harvey (2013). The model then remains easy to estimate via standard maximum likelihood methods. It is also known note score-driven dynamics possess information theoretic optimality properties and yield updates of the parameters that (in expectation) improve the fit of the model to the data (as measured in the so-called Kullback-Leibler divergence); see Blasques et al. (2015) and Creal et al. (2020).

To define the score-driven dynamics for $\boldsymbol{R}_t$ and $\boldsymbol{\Sigma}_t$, we gather all time-varying spatial parameters as well as the volatilities into the vector $\boldsymbol{f}_t$. In particular, we set

$$\boldsymbol{f}_t = (\boldsymbol{R}_{11,t}, \dots, \boldsymbol{R}_{NN,t}, \log \boldsymbol{\Sigma}_{11,t}, \dots, \log \boldsymbol{\Sigma}_{NN,t})^\top, \tag{2}$$

where $\boldsymbol{R}_{i,i,t}$ and $\boldsymbol{\Sigma}_{i,i,t}$ are the ith diagonal elements of $\boldsymbol{R}_t$ and $\boldsymbol{\Sigma}_t$, respectively. As $\boldsymbol{\Sigma}_{i,i,t} = \exp(\boldsymbol{f}_{i+N,t})$, we ensure that the (time-varying) variances $\boldsymbol{\Sigma}_{i,i,t}$ of the shocks $\boldsymbol{\varepsilon}_{i,t}$ are always positive.[1] The spatial model retains its network stability if the spatial spillovers die out. For this, we only require $\boldsymbol{R}_t\boldsymbol{W}_t$ to have all eigenvalues inside the unit circle. Note that this still allows for $\boldsymbol{R}_{i,i,t} > 1$ for specific network players i, as long as the maximum eigenvalue of $\boldsymbol{R}_t\boldsymbol{W}_t$ remains below one. The latter depends on all elements of $\boldsymbol{R}_t$ and $\boldsymbol{W}_t$, and not on one specific $\boldsymbol{R}_{i,i,t}$ only. The fact that we allow $\boldsymbol{R}_{i,i,t}$ to move outside the unit interval therefore provides substantial flexibility to the model. This comes on top of the flexibility provided by allowing the diagonal elements of $\boldsymbol{R}_t$ to be different in the first place compared to the scalar model $\boldsymbol{R}_t = \rho_t \cdot \mathbf{I}_N$ of Blasques et al. (2016).

[1] Other parameterization choices are also possible. One may for instance choose to model the logit transforms $\log(\boldsymbol{R}_{i,i,t}/(1-\boldsymbol{R}_{i,i,t}))$ of $\boldsymbol{R}_{i,i,t}$ rather than $\boldsymbol{R}_{i,i,t}$ itself to ensure that $\boldsymbol{R}_{i,i,t} \in [0,1]$ for all values of $\boldsymbol{f}_t$. Though intuitive, such reparameterizations may come at a considerable cost. In fact, we show in this paper that using the logit transforms for $\boldsymbol{R}_{i,i,t}$ is actually a bad idea if there is heterogeneity in spillover sensitivity: it unnecessarily restricts the model's ability to capture the dynamics in the data and leads to biased estimates, as some $\boldsymbol{R}_{i,i,t}$ may go outside the 0–1 range without jeopardizing the spatial stability of the model.

Using our definition of $\boldsymbol{f}_t$, the score-driven dynamics are given by

$$\boldsymbol{f}_{t+1} = \boldsymbol{\omega} + \boldsymbol{B}\,\boldsymbol{f}_t + \boldsymbol{A}\,\boldsymbol{s}_t, \tag{3}$$

$$\begin{aligned}\boldsymbol{s}_t &= \frac{\partial \log p_{\boldsymbol{y}}\left(\boldsymbol{y}_t \mid \boldsymbol{f}_t; \boldsymbol{\Sigma}_t, \nu\right)}{\partial \boldsymbol{f}_t} \\ &= \underbrace{\frac{\partial \log p_{\boldsymbol{\varepsilon}}\left(\boldsymbol{\Sigma}_t^{-1/2}\left(\boldsymbol{y}_t - \boldsymbol{R}_t\boldsymbol{W}_t\boldsymbol{y}_t - \boldsymbol{X}_t\boldsymbol{\beta}\right)\ ; \boldsymbol{\Sigma}_t, \nu\right)}{\partial \boldsymbol{f}_t}}_{\text{part (i)}} \\ &\quad \underbrace{-\tfrac{1}{2}\frac{\partial \log|\boldsymbol{\Sigma}_t|}{\partial \boldsymbol{f}_t}}_{\text{part (ii)}} + \underbrace{\tfrac{1}{2}\frac{\partial \log\left|(\mathbf{I}_N - \boldsymbol{R}_t\boldsymbol{W}_t)^2\right|}{\partial \boldsymbol{f}_t}}_{\text{part (iii)}},\end{aligned} \tag{4}$$

where we use unit scaling in the sense of Creal et al. (2013). The derivations can be found in the appendix. Equation (4) reveals that the score dynamics of volatilities and spatial spillover parameters contains three components: (i) a part related to the density of $\boldsymbol{\varepsilon}_t$ affecting both $\boldsymbol{R}_t$ and $\boldsymbol{\Sigma}_t$, (ii) a part related to the Jacobian of the transformation from $\boldsymbol{\varepsilon}_t$ to $\boldsymbol{y}_t$ and affecting only $\boldsymbol{\Sigma}_t$, and (iii) a part related to the same Jacobian and accounting for the simultaneity bias in the spatial lag set-up of the model, thus affecting only $\boldsymbol{R}_t$. These three components are worked out in detail below.

Rather than assuming that the errors $\boldsymbol{\varepsilon}_t$ are normally distributed, we assume that $\boldsymbol{\varepsilon}_t$ follows a fat-tailed Student's t distribution with zero mean, covariance matrix $\boldsymbol{\Sigma}_t$, and ν degrees of freedom,

$$p_{\boldsymbol{\varepsilon}}\left(\boldsymbol{\varepsilon}_t\ ; \boldsymbol{\Sigma}_t, \nu\right) = \frac{\Gamma\left(\frac{1}{2}(\nu+N)\right)}{\Gamma\left(\frac{1}{2}\nu\right)\ |(\nu-2)\pi\boldsymbol{\Sigma}_t|^{1/2}}\ \left(1 + \boldsymbol{\varepsilon}_t^{\top}\boldsymbol{\Sigma}_t^{-1}\boldsymbol{\varepsilon}_t/(\nu-2)\right)^{-0.5(\nu+N)}. \tag{5}$$

The normal distribution is recovered as a special case for $\nu \to \infty$. The problem with the normal distribution, however, is that it does not allow for incidentally large observations and fat tails in the data, which is particularly problematic for financial economic data as in our application later in the paper. In addition, the Student's t distribution produces robust dynamics for the time-varying parameters $\boldsymbol{R}_t$ and $\boldsymbol{\Sigma}_t$ via the score-driven updates in (4). To see the latter, we show in the appendix that for the Student's t distribution equation (4) reduces to

$$\boldsymbol{s}_{i,t} = \begin{cases} w_t\ \boldsymbol{\Sigma}_{i,i,t}^{-1}\boldsymbol{y}_{i,t}^{\star}\boldsymbol{e}_{i,t} - \left(\boldsymbol{W}_t\left(\mathbf{I}_N - \boldsymbol{R}_t\boldsymbol{W}_t\right)^{-1}\right)_{i,i} & \text{for } i = 1,\ldots,N, \\ \frac{1}{2}\,w_t\,\boldsymbol{\Sigma}_{i-N,i-N,t}^{-1}\boldsymbol{e}_{i-N,t}^2 - \frac{1}{2} & \text{for } i = N+1,\ldots,2N, \end{cases} \tag{6}$$

where $\boldsymbol{s}_{i,t}$ is the ith element of $\boldsymbol{s}_t$, and

$$\boldsymbol{y}_t^\star = (\boldsymbol{y}_{1,t}^\star, \ldots, \boldsymbol{y}_{N,t}^\star)^\top = \boldsymbol{W}_t \boldsymbol{y}_t, \tag{7}$$

$$\boldsymbol{e}_t = (\boldsymbol{e}_{1,t}, \ldots, \boldsymbol{e}_{N,t})^\top = \boldsymbol{y}_t - \boldsymbol{R}_t \boldsymbol{W}_t \boldsymbol{y}_t - \boldsymbol{X}_t \boldsymbol{\beta}, \tag{8}$$

$$w_t = \left(1 + \frac{N+2}{\nu-2}\right) \Big/ \left(1 + \frac{\boldsymbol{e}_t^\top \boldsymbol{\Sigma}_t^{-1} \boldsymbol{e}_t}{\nu-2}\right). \tag{9}$$

For the normal distribution, $w_t = 1$ in (6). For the Student's t distribution with $\nu < \infty$, however, the weight w_t provides a robustness feature to the time-varying parameter dynamics: if an observation $\boldsymbol{y}_t$ is an incidental outlier or influential observation with a large $\boldsymbol{e}_t$, the weight w_t tends to zero. Such observations thus receive less impact on the volatility and spatial correlation dynamics. This is a distinct advantage of the current model; see also similar features for other location and scale models in for instance Creal et al. (2013) and Harvey and Luati (2014).

The two scores in (6) have an intuitive interpretation. The first set of scores for $i = 1, \ldots, N$ relates to the spatial correlation parameters $\boldsymbol{R}_{i,i,t}$. These scores consist of two terms. The first term is the regressor weighted standardized error term $\boldsymbol{e}_{i,t}$, where the regressor $\boldsymbol{y}_{i,t}^\star$ is the ith element of the dependent variable $\boldsymbol{y}_t$ pre-multiplied by the spatial weights matrix $\boldsymbol{W}_t$. As $\boldsymbol{R}_{i,i,t}$ can be seen as a (spatial) regression parameter, this part of the score adjusts the parameter upwards or downwards depending on whether the most recent observation lies below or above the estimated regression line at the previous point in time. The second term in the equations in (6) corrects for the simultaneity bias in the regression specification due to the endogeneity of $\boldsymbol{y}_t$. The endogeneity correction naturally becomes smaller if either $\boldsymbol{R}_t$ or $\boldsymbol{W}_t$ lie closer to zero, i.e., if the endogeneity problem is less. The second set of equations in (6) relates to the volatility parameters $\log \boldsymbol{\Sigma}_{i,i,t}$ and are more familiar from the literature, see for instance Creal et al. (2011). We recognize the GARCH type pattern for the volatilities: $\log \boldsymbol{\Sigma}_{i,i,t}$ reacts to standardized squared error terms $\boldsymbol{e}_{i,t}^2 / \boldsymbol{\Sigma}_{i,i,t}$. If the weighted ($w_t$) squared errors exceed their expectation $\boldsymbol{\Sigma}_{i,i,t}$, the volatility parameters are adjusted upwards. As mentioned before, the weights w_t due to the use of the Student's t distribution ensure that the volatility dynamics are robust to incidental outliers and fat tails.

2.3 Estimation

Score-driven models can easily be estimated by maximum likelihood methods via a standard prediction error decomposition. Gathering all static parameters in the vector $\boldsymbol{\theta} = (\boldsymbol{\beta}, \nu, \boldsymbol{\omega}, \boldsymbol{A}, \boldsymbol{B})$, we

obtain the objective function

$$\ell(\boldsymbol{\theta}) = \sum_{t=1}^{T} p_{\boldsymbol{y}}(\boldsymbol{y}_t \mid \boldsymbol{f}_t, \boldsymbol{\theta}) \equiv \sum_{t=1}^{T} p_{\boldsymbol{y}}(\boldsymbol{y}_t \mid \boldsymbol{R}_t, \boldsymbol{\Sigma}_t, \nu). \tag{10}$$

To compute the likelihood, one proceeds as follows. Given a value of $\boldsymbol{\theta}$ and an initial value $\boldsymbol{f}_1$, one obtains the time-varying parameter values $\boldsymbol{f}_t$ for all times $t = 1, \ldots, T$ using the recursion (3). With these values of $\boldsymbol{f}_t$, we obtain the values of $\boldsymbol{R}_t$ and $\boldsymbol{\Sigma}_t$ using equation (2). These can then directly be plugged into (10) to obtain the value of the log-likelihood function. The initial $\boldsymbol{f}_1$ is obtained by estimating a static version of the model on the initial 2 years of observations and setting $\boldsymbol{f}_1$ to the estimates of the spatial correlation parameters and log error variances. If a transformation was applied in equation (2), of course the inverse of the same transformation is first applied to these static initial estimates.

We obtain the maximum likelihood estimator as $\hat{\boldsymbol{\theta}}_T = \arg\max_{\boldsymbol{\theta}} \ell(\boldsymbol{\theta})$. The covariance matrix of $\hat{\boldsymbol{\theta}}_T$ can be estimated in the usual way as

$$\hat{\boldsymbol{V}}_T = \hat{\boldsymbol{H}}_T^{-1} \cdot \hat{\boldsymbol{J}}_T \cdot \hat{\boldsymbol{H}}_T^{-1}, \quad \hat{\boldsymbol{J}}_T = \sum_{t=1}^{T} \frac{\mathrm{d} p_{\boldsymbol{y}}(\boldsymbol{y}_t \mid \boldsymbol{f}_t, \hat{\boldsymbol{\theta}}_T)}{\mathrm{d}\boldsymbol{\theta}} \frac{\mathrm{d} p_{\boldsymbol{y}}(\boldsymbol{y}_t \mid \boldsymbol{f}_t, \hat{\boldsymbol{\theta}}_T)}{\mathrm{d}\boldsymbol{\theta}^\top}, \quad \hat{\boldsymbol{H}}_T = -\frac{\partial^2 \ell(\hat{\boldsymbol{\theta}}_T)}{\partial\boldsymbol{\theta}\partial\boldsymbol{\theta}^\top}, \tag{11}$$

where the computation of the outer-product-of-gradients $\hat{\boldsymbol{J}}_T$ uses the total rather than the partial derivatives. If the model is correctly specified, $\hat{\boldsymbol{H}}_T = \hat{\boldsymbol{J}}_T$ and the covariance matrix collapses to $\hat{\boldsymbol{V}}_T = -\hat{\boldsymbol{H}}_T^{-1}$

2.4 Simulation evidence

To investigate the properties of the new model and the effects of heterogeneity in the spatial autoregressive parameters, we report the results of a small simulation experiment. The experiment is set up as follows. We consider a data generating process (dgp) with dynamic, heterogeneous spatial parameters $\boldsymbol{R}_t$. We use a setting with fat-tailed structural shocks ($\nu = 5$), no regressors ($\boldsymbol{\beta} = 0$), and no heteroskedasticity ($\boldsymbol{\Sigma}_t = \boldsymbol{\Sigma}$) with $N = 4$. We simulate around 600 observations, similar in magnitude to the number of time series observations in the application. For $\boldsymbol{W}_t$, we use the row-normalized empirical spatial weight matrices $\boldsymbol{W}_t$ for Germany, France, Italy, and the Netherlands from Section 4. For concreteness, we set $\boldsymbol{A} = 0.07 \cdot \mathbf{I}_N$, $\boldsymbol{B} = 0.9 \cdot \mathbf{I}_N$, and $(\mathbf{I}_N - \boldsymbol{B})^{-1}\boldsymbol{\omega} = (0.45, 0.65, 0.90, 0.35)^\top$, where the latter is the unconditional mean of the diagonal elements of $\boldsymbol{R}_t$. Qualitatively similar results are obtained for other parameter settings.

We estimate four different models: a static scalar model (ρ), a dynamic scalar model (ρ_t), a static diagonal model ($\boldsymbol{R}$), and a dynamic diagonal model ($\boldsymbol{R}_t$). This allows us to clearly see the

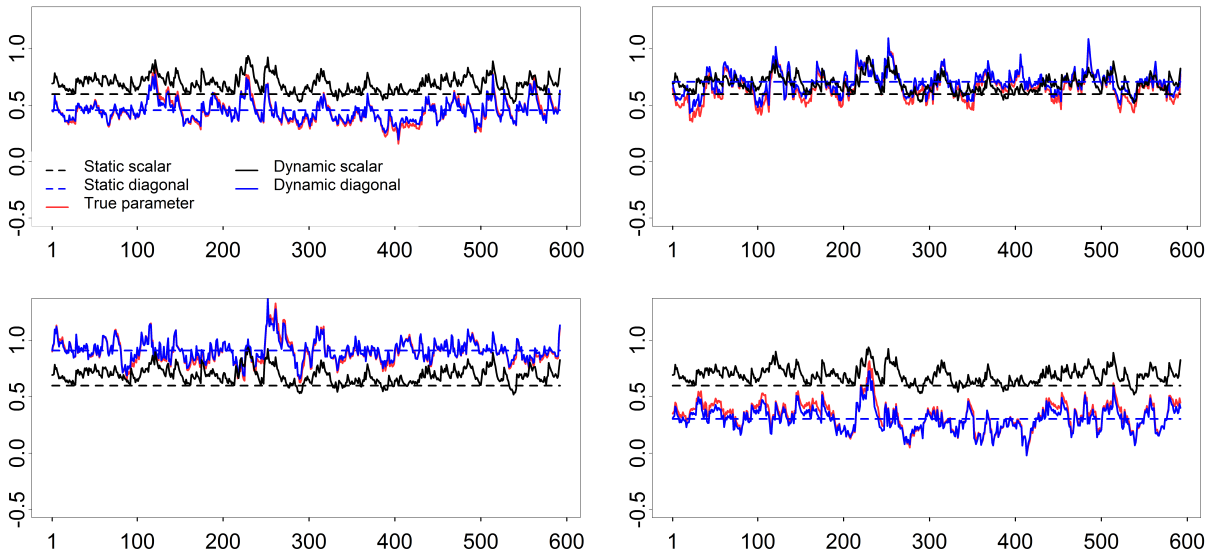

Figure 1: Simulated true and fitted spatial dependence parameters

Each panel shows the simulated and estimated paths of one out of $N = 4$ spatial autoregressive parameters. The true data generating process has heterogeneous time varying spatial parameters with unconditional means equal to 0.45 (top-left), 0.65 (top-right), 0.90 (bottom-left), and 0.35 (bottom right), respectively. The four models estimated are the static scalar spatial autoregression ($\boldsymbol{R}_t = \rho \cdot \mathbf{I}_N$), the static diagonal model ($\boldsymbol{R}_t = \boldsymbol{R}$), the dynamic scalar model of Blasques et al. (2016) ($\boldsymbol{R}_t = \rho_t \cdot \mathbf{I}_N$), and the new diagonal spatial model (diagonal $\boldsymbol{R}_t$).

separate contributions of dynamics and heterogeneity. Figure 1 reports the results for a typical simulation. The simulated time-variation and heterogeneity are actually quite modest compared to the empirical patterns found in the data in Section 4.

Figure 1 shows that the correctly specified model (solid blue curve) captures the movements in the dgp (solid red) highly accurately for sample sizes similar to those in our empirical application.[2] The static version of the model $\boldsymbol{R}_t = \boldsymbol{R}$ (dashed blue) with heterogeneity but without dynamics still captures the unconditional level of the true time-varying spatial correlations, but misses all of the significant dynamics of sometimes up to size 0.4. The standard static scalar spatial autoregression of Anselin (2009) with $\boldsymbol{R}_t = \rho \cdot \mathbf{I}_N$ fares even worse. It has to balance the different levels of the spatial autocorrelations both in the cross section and over time and therefore lands at some sort of average spatial autocorrelation of ρ around 0.55 to 0.6 (dashed black).

We see a similar bias for the dynamic scalar spatial regression model (solid black) of Blasques et al. (2016). The true spatial correlations (in red) are below the black solid curve for the top-left and bottom-right panels, whereas it is above and on top of the black curve in the other two panels. Again, given the heterogeneity in the true spatial correlations, the scalar model can only

[2]Additional unreported simulations show that the new model can also adequately track the true model parameters even in cases where the statistical model is misspecified. This is in line with the theoretical results in Blasques et al. (2015) and Creal et al. (2020).

take some kind of average of these, both in terms of the overall level and in terms of the specific dynamics over time. For the latter, we note for instance in the bottom-left graph the peaks of similar magnitude in the black curve around observations 230 and 260, respectively. The true (in red) dynamics of $\boldsymbol{R}_{i,i,t}$ for this cross-sectional unit, however, only have a peak around observation 260, and not around time 230. The latter peak in the black curve appears more attributable to the bottom-right cross-sectional unit, which clearly peaks around time 260, but not around the earlier time 230. As all heterogeneous dynamics of all series have to be captured by one single ρ_t for this model, a mixed-up message emerges about what is actually happening in the data. Our new model with heterogeneous, diagonal $\boldsymbol{R}_t$ avoids all these issues and captures the variety of dynamics much better.

3 Data

We apply the model to analyze the network dynamics of sovereign systemic risk in the euro-zone. We consider seven countries: Germany, France, Ireland, Italy, Netherlands, Portugal, and Spain. Our sample period spans December 10, 2009 until July 2, 2020. As our dependent variable y_t we consider the changes of 5-year government yield spreads. The yield spread is defined as the difference between the Euro-denominated 5-year government bond yield and the 5-year EONIA OIS rate to concentrate on the credit risk component of sovereign bonds. Later, we also provide a robustness analysis using a 1-year rather than 5-year maturity, as well as using CDS spreads rather than bond yield spreads. The sample contains 543 weekly observations for each country. Data are taken from Datastream and Bloomberg.

We base our main analysis on changes in 5-year government yield spreads rather than on log returns. Log returns can lead to peculiar results during our sample period, as spreads near zero can result in log returns on these spreads being very large. For instance, this may lead to Germany being the most volatile country in the sample. By taking differences rather than log differences, these problems are avoided and the results are much more intuitive, for instance Germany becoming one of the safer countries in the sample. We also base our main analysis on bond yields rather than CDS spreads (though we have a robustness analysis with CDS spreads as well). Particularly during the later years in the sample, sovereign CDSs are less liquidly traded compared to their underlying bonds. As a result, all CDS spreads hover more closely to zero with little variation and instability in the estimates of the spatial correlation parameters. Again, these issues are avoided by working with the bond yield data instead.

Figure 2 presents the government yield spreads. All countries in our sample tend to co-move especially during the 2010–2012 European sovereign debt crisis, except for Germany and to some

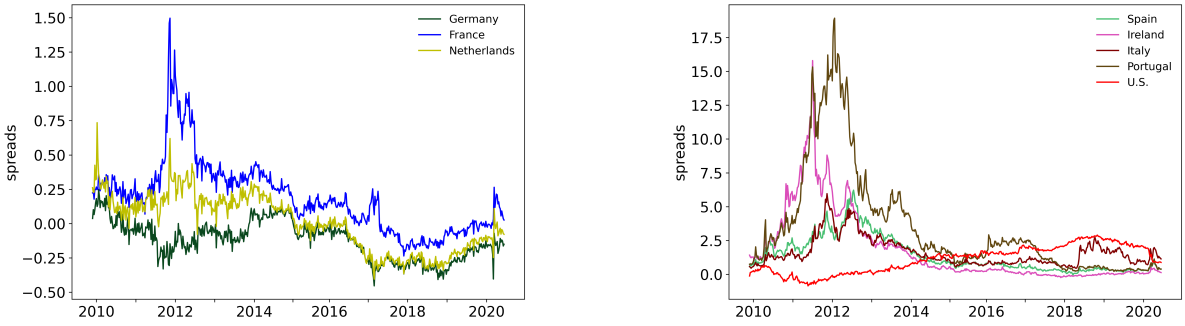

Figure 2: Government bond yield spreads of seven Eurozone sovereigns and the U.S.

Weekly Euro-denominated 5-year government yield spreads of seven European countries and the United States from December 2009 - July 2020.

extent the Netherlands. Whereas most yields go up during the crisis, those of Germany go down, Germany acting as an anchor and safe-haven for the euro during that time. Note that the right-hand panel has a different vertical scale, indicating that the countries in that panel have much higher government yield spread levels compared to the countries in the left-hand panel. This makes sense, as these were precisely the countries that were at the center of the crisis.

Table 1 reports summary statistics. We see high volatilities for countries such as Portugal, Ireland, Italy and Spain compared to Germany. The kurtosis is high for all series, indicating that the data are (unconditionally) peaked and that a combination of volatility clustering and conditional non-normality may be called for in the model. Note that the model proposed in this paper indeed accommodates both.

We use three control variables from the literature. To control for economic conditions, we include the (log) returns in each country's main stock index as well as the slope of the term structure (gpvernment bond yield 10-year minus 1-year) for each country. We also control for various measures of market stress by including the changes in the VSTOXX index. The VSTOXX index measures volatility in options markets and is therefore forward looking measures of market stress and investor sentiment. It also relates to the local Eurozone developments and the risk perceptions and appetite.

As a final ingredient of the model, we require data for the spatial weight matrices $\boldsymbol{W}_t$. We choose domestic banks cross-border exposures as in Tonzer (2015) using data extracted from the BIS website.[3] A small number of missing values are back-filled by the last available observations. The consolidated statistics in the BIS database cover the positions of international bank cross border holdings and thus provide a measure of interconnectedness of the financial system in the

[3] https://stats.bis.org/, retreived July 17, 2020.Like Blasques et al. (2016), we use the immediate counterparty risk measure of banking groups' country risk exposures.

Table 1: Summary statistics 5-year government bonds

This table lists descriptive statistics of changes of 5-year government yield spreads of seven European countries and the United States. The yield spread is defined as the difference between the 5-year government bond yield and the 5-year EONIA OIS rate. In addition, we list summary statistics of stock returns and changes in the VSTOXX index and term spread. The term spread is computed as the absolute change between the 10-year and 1-year government bond yield. All variables are weekly from December 10, 2009 until July 2, 2020.

	mean	s.d.	med	min	max	skew	kurt
5 year gov bond spread changes							
Germany	0.000	0.052	0.001	-0.20	0.33	0.30	7.38
Spain	0.000	0.180	-0.003	-1.07	0.82	-0.22	8.64
France	0.000	0.069	-0.001	-0.64	0.35	-0.95	19.94
Ireland	-0.002	0.361	0.001	-3.07	2.76	-0.90	29.65
Italy	0.001	0.196	-0.001	-0.93	0.99	0.52	8.29
Netherland	-0.001	0.062	0.000	-0.27	0.41	0.72	10.90
Portugal	0.000	0.505	-0.004	-3.31	3.95	0.30	21.44
U.S.	0.002	0.088	0.004	-0.40	0.27	-0.43	4.50
Stock index returns							
Germany	0.001	0.029	0.004	-0.22	0.10	-1.31	11.62
Spain	-0.001	0.032	0.002	-0.23	0.10	-0.92	8.54
France	0.000	0.028	0.003	-0.22	0.10	-1.28	11.24
Ireland	0.001	0.026	0.003	-0.20	0.08	-1.47	11.18
Italy	0.000	0.033	0.002	-0.26	0.10	-1.34	11.20
Netherlands	0.001	0.026	0.003	-0.20	0.09	-1.50	12.59
Portugal	-0.001	0.029	0.001	-0.20	0.07	-1.11	7.92
Gov. yield spread changes (10-year - 1-year)							
Germany	-0.004	0.081	-0.011	-0.278	0.523	0.994	7.44
Spain	-0.005	0.224	0.000	-3.732	1.175	-8.107	144.5
France	-0.004	0.083	-0.007	-0.335	0.578	0.838	8.11
Ireland	-0.005	0.279	-0.012	-2.283	2.628	0.790	30.65
Italy	-0.002	0.154	-0.008	-0.855	1.125	1.022	14.74
Netherlands	-0.006	0.108	-0.009	-0.890	0.828	-0.112	22.57
Portugal	-0.003	0.431	-0.007	-2.475	2.536	-0.035	13.00
Control variable							
Δ VSTOXX	-0.001	3.906	-0.150	-16.98	31.31	1.68	16.81

Eurozone. Financial system interconnectedness can be regarded as one of the prominent determinants for sovereign credit risk spillovers given the bail-out incentive of governments for their local banking sector, and its potential effect on government creditworthiness. The quarterly data on cross-exposures are converted to weekly values by taking the latest value of the BIS data available in that week. We lag the entries by two quarters to prevent the use of future information in $\boldsymbol{W}_t$. The spatial weight matrices are row-normalized.

4 Empirical application

In this section we discuss our empirical results. Parameter estimates of the different models can be found in Section 4.1, while Section 4.2 contains their risk spillover implications.

4.1 Spatial dependence dynamics in the euro zone

Table B.3 presents the parameter estimates for four alternative model specifications. The first two columns relate the the static and dynamic model with homogeneous spatial dependence parameter ρ_t. The last two columns correspond to the models with heterogeneous spatial autoregressive parameters $\boldsymbol{R}_t$. For the dynamic version of this model, we use a common parameter $\boldsymbol{B} = \beta \cdot \mathbf{I}_N$, but heterogeneous adjustment speeds for the spatial parameters, $\boldsymbol{A} = \text{diag}(\alpha_1, \ldots, \alpha_N, \alpha_{vol}, \ldots, \alpha_{vol})$, with α_i the speed of adjustment of $\boldsymbol{R}_{i,i,t}$, and α_{vol} the common speed of adjustment of the volatilities. Allowing for heterogeneous volatility adjustment parameters does not impact out main results.

Allowing for heterogeneous spatial spillover parameters considerably improves the statistical fit of the model. The maximized log-likelihood increases by roughly 195 points in the static case, and by around 216 points for the dynamic case. Heterogeneity in spatial dynamics thus appears a key property in the data. Allowing for dynamic rather than static spatial dependence also increases the fit of the model. The log-likelihood increases by 42 points in the scalar case, and by 63 points for the heterogeneous model. The value-added of the dynamics thus comes out more clear in the heterogeneous case. This is in line with the simulation results from Section 2.4: not only the levels, but also the dynamic patters are corrupted if we incorrectly pool spillover parameters across countries.

The importance of both the heterogeneity and dynamics clearly shows in the plots of ρ_t and $\boldsymbol{R}_{i,i,t}$ in Figure 3. The plots are easily obtained by evaluating $\boldsymbol{f}_t$ for $t = 1, \ldots, T$ at the maximum likelihood estimate $\hat{\boldsymbol{\theta}}$, and then inserting $\boldsymbol{f}_t(\hat{\boldsymbol{\theta}})$ into equation (2) to obtain estimated volatilities and spatial spillover parameters. The left-hand panel shows the results for the scalar model. The static estimate of ρ of slightly below 0.5 corresponds to the long-run average of the dynamic scalar ρ_t. The variation of ρ_t over time is quite modest between $\rho_t = 0.2$ and $\rho_t = 0.7$.

The picture changes dramatically if we consider the heterogeneous spatial spillover parameters $\boldsymbol{R}_{i,i,t}$ in the right-hand panel of the figure. Note that both panels have the same vertical scale. Whereas the scalar ρ_t varied between 0.2 and 0.7, the $\boldsymbol{R}_{i,i,t}$ vary between values below 0 up to 1.5. There are clearly two contributions to this. First, as we see for the static version of the heterogeneous model, static spillover parameters $\boldsymbol{R}_{i,i}$ considerably fan out across countries and range between a low value around 0 for Germany, to a high value of 1.1 for Italy. Note that this

Table 2: Parameter estimates: 5-year bond yields

This table reports the estimated parameters of four spatial dependence models, applied to weekly first differences in the spread between 5-year government bond yields and the 5-year EONIA. Results are for seven Eurozone countries. Robust (Huber sandwich) standard errors are reported in parentheses. The models are based on Student's t distributed disturbances with time-varying heteroscedasticity as in model (1)–(4). For the diagonal models, we have $\boldsymbol{B} = \beta \cdot \mathbf{I}_N$ and $\boldsymbol{A} = \text{diag}(\alpha_1, \ldots, \alpha_N, \alpha_{vol}, \ldots, \alpha_{vol})$ We report the maximum log-likelihood value (LogLike) and AIC(Akaike information criterion). The sample runs from December 2009 - July 2020. The table is continued on the next page.

	Static Scalar	Dynamic Scalar	Static Diagonal	Dynamic Diagonal
Panel A: Spatial dependence parameters				
ω/ω_{GE}	0.463	0.009	0.074	-0.001
	(0.022)	(0.005)	(0.031)	(0.002)
ω_{SP}			0.628	0.010
			(0.060)	(0.006)
ω_{FR}			0.341	0.005
			(0.026)	(0.003)
ω_{IR}			0.819	0.012
			(0.043)	(0.006)
ω_{IT}			1.111	0.030
			(0.108)	(0.012)
ω_{NE}			0.682	0.012
			(0.038)	(0.004)
ω_{PO}			0.898	0.014
			(0.069)	(0.007)
α/α_{GE}		0.005		0.009
		(0.001)		(0.003)
α_{SP}				0.039
				(0.014)
α_{FR}				0.009
				(0.003)
α_{IR}				0.007
				(0.009)
α_{IT}				0.089
				(0.038)
α_{NE}				0.016
				(0.008)
α_{PO}				0.016
				(0.014)
β_ρ		0.982		0.985
		(0.010)		(0.007)
Panel B: Volatility and control parameters				
(see next page)				

does not impair the spatial instability of the model: the maximum eigenvalue of $\boldsymbol{R}_t\boldsymbol{W}_t$ is still below 1 at all times. The effect of this large variation in spatial dependence parameters for our assessment of the risk dynamics is also considerable, and we come back to that in the next subsection. Second,

(Table 2 continued)

	Static Scalar	Dynamic Scalar	Static Diagonal	Dynamic Diagonal
Panel B: Volatility and control parameters				
α_{vol}	0.276	0.271	0.289	0.277
	(0.026)	(0.026)	(0.027)	(0.027)
β_{vol}	0.998	0.998	0.998	0.998
	(0.002)	(0.002)	(0.002)	(0.002)
ν	3.483	3.540	4.015	4.108
	(0.326)	(0.334)	(0.412)	(0.416)
Δ VSTOXX	0.004	0.010	-0.001	0.004
	(0.032)	(0.029)	(0.030)	(0.026)
Δ term spread	0.058	0.057	0.037	0.042
	(0.049)	(0.045)	(0.046)	(0.042)
local stock	-0.022	-0.021	-0.019	-0.019
	(0.011)	(0.010)	(0.010)	(0.009)
logLik	4454	4496	4649	4712
AIC	-8865	-8946	-9244	-9353

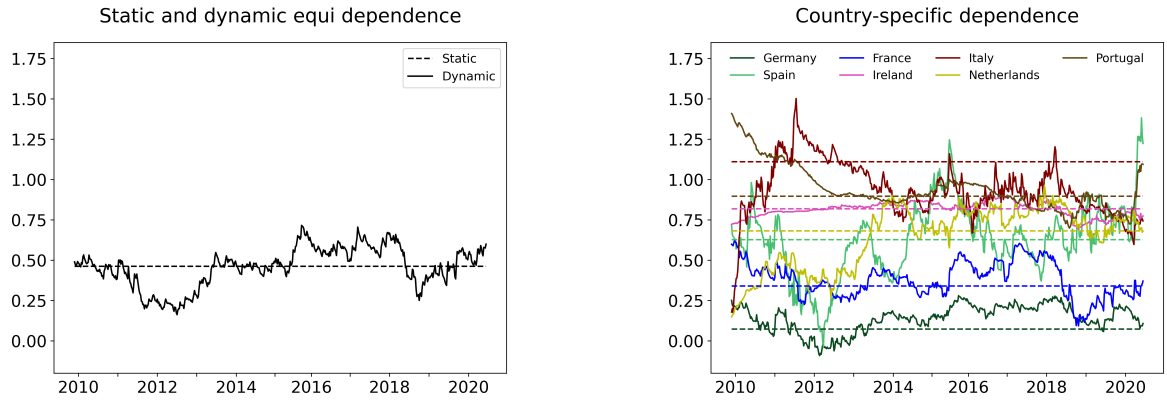

(a) (b)

Figure 3: Filtered spatial autoregressive parameters

This figure depicts fitted dependencies from four different models, applied to Euro-denominated 5-year government bond yield spreads of seven European countries. The top figure depicts the fixed and time-varying equi-spatial dependencies, whereas the bottom figure shows the heterogeneous fixed and time-varying dependencies through time. The sample runs from December 2009 - July 2020.

we see that the time-variation contributes to the variability of $\boldsymbol{R}_{i,i,t}$. For instance, $\boldsymbol{R}_{i,i,t}$ for Italy ranges from a low 0.25 at the start, to a high 1.5 in the midst of the European sovereign debt crisis.

We also see that allowing for heterogeneity substantially impacts the dynamics of ρ_t versus $\boldsymbol{R}_{i,i,t}$. Whereas the scalar ρ_t shows mild variation over time between roughly 0.2 and 0.7 without any differences for the Eurozone countries, the $\boldsymbol{R}_{i,i,t}$ dynamics are much more varied. Some coun-

tries show a large time-variation, with quite different peaks and troughs, whereas other countries are much more stable over time. For instance, the $\boldsymbol{R}_{i,i,t}$ for Germany tightly hovers between -0.1 and 0.25. The fact that it becomes slightly negative at times, corroborates Germany's role as an anchor and stabilizer for the Eurozone, a feature that is not clear from the scalar homogeneous model, nor from the static version of the heterogeneous model. We also see that ρ_t in the scalar model remains rather stable until mid-2011: it averages the highly opposite upward movements of Italy and to a lesser extent Ireland and the Netherlands, versus the downward movements of Spain, Portugal, France, and Germany. Only around the time that Italy also starts its descent, the scalar ρ_t starts to react and go mildly down. The descent of Italy's $\boldsymbol{R}_{i,i,t}$ comes after a range of non-standard support measures by the following the financial crisis. One should however be cautious in over-interpreting the dynamics of ρ_t or $\boldsymbol{R}_{i,i,t}$ on their own: in terms of systemic risk implications, the $\boldsymbol{R}_{i,i,t}$ mix with the known spatial weight matrix $\boldsymbol{W}_t$ and the time-varying volatilities $\boldsymbol{\Sigma}_t$ to form spatial spillovers. We come back to this in the next subsection, where we interpret all these components jointly.

One of the striking patterns in Figure 3b is the repeated exceedance of $\boldsymbol{R}_{i,i,t}$ above the threshold 1 for countries like Italy, Portugal, and Spain. Again, we stress that the model remains still stable given that $\boldsymbol{R}_t\boldsymbol{W}_t$ is never explosive, though $\boldsymbol{R}_t$ itself may be. A second highlight in both Figure 3b and Table B.3 is the importance of allowing for differences in adjustment speeds α_i on top of the differences in the long-run levels of $\boldsymbol{R}_{i,i,t}$ Countries like Germany, France, and Ireland have a low α_i, indicating that time-variation in $\boldsymbol{R}_{i,i,t}$ for those countries is modest in size. By contrast, other countries such as Spain and particularly Italy require a much larger value of α_i, resulting in a wider range of variation for $\boldsymbol{R}_{i,i,t}$. Not allowing for this type of heterogeneity would again substantially distort the empirical results and result in too much stability of $\boldsymbol{R}_t$, as the model would have to average the different adjustment speeds. Note that all β parameters for the $\boldsymbol{R}_{i,i,t}$ dynamics are pooled. Differentiating these does not increase the likelihood by much, and all persistence parameters β_i remain close to one, such that little is lost by pooling these as opposed to the result for the α_is.

Some final highlights can be found in Panel B of Table B.3. We see that none of the control variables is statistically significant, a feature that we further corroborate in our robustness analyses in Section 5. We also see that it is important to allow for fat tails and volatility clustering. The persistence of volatility is high with a β_{vol} close to one, whereas α_{vol} is also strongly significant.[4] The degrees of freedom parameter ν is also significant and actually quite low given that we also control for volatility clustering: this indicates that government bond yield spreads changes have fat

[4]Note that in a score-driven model we need not have $\alpha_{vol} + \beta_{vol} < 1$ as in a GARCH context, but rather $\beta_{vol} < 1$ only.

tails and that even 4th order (conditional) moments of government bond yield spreads changes may not exist. Again, this does not result in problems for our score-driven model, unlike for a standard GARCH model where typically 4th order moments are needed for consistency; see Blasques et al. (2021) for details on the asymptotics of score-driven models. Also note that the the heterogeneity and dynamics resolve part of the fat-tailedness problem, as the estimate of ν increases somewhat from 3.5 to 4.

Summarizing, the statistical improvements by allowing for heterogeneous and time-varying spatial spillovers in European sovereign credit risk changes is statistically important. It also results in substantial new insights in the spatial spillover dynamics compared to models that either lack time-varying parameters or impose homogeneity in spatial spillovers. We now confirm these findings by looking in more detail to the model's systemic risk measurement implications.

4.2 Systemic risk spillovers in the Eurozone

In this section, we analyze how sovereign credit risk percolates across countries in our spatial model set-up. Though we have seen the differences in spatial dynamics for the scalar ρ_t versus the heterogeneous $\boldsymbol{R}_t$ specifications in the previous subsection, such differences cannot be extrapolated immediately into risk spillover differences. The main reason for this is that the immediate spillover is not only composed of $\boldsymbol{R}_t$, but of the composite $\boldsymbol{R}_t$ and $\boldsymbol{W}_t$. The full reduced form effect is a composite of $\mathbf{I}_N + \boldsymbol{R}_t\boldsymbol{W}_t + (\boldsymbol{R}_t\boldsymbol{W}_t)^2 + \ldots = (\mathbf{I}_N - \boldsymbol{R}_t\boldsymbol{W}_t)^{-1}$. We can see the latter by looking at the spatial impulse responses and rewriting (1) as

$$\begin{aligned}
&\boldsymbol{y}_t = \boldsymbol{R}_t\boldsymbol{W}_t\boldsymbol{y}_{t-1} + \boldsymbol{X}_t\boldsymbol{\beta} + \boldsymbol{\varepsilon}_t \quad \Leftrightarrow \quad (\mathbf{I}_N - \boldsymbol{R}_t\boldsymbol{W}_t)\,\boldsymbol{y}_t = \boldsymbol{X}_t\boldsymbol{\beta} + \boldsymbol{\varepsilon}_t \quad \Leftrightarrow \\
&\boldsymbol{y}_t = (\mathbf{I}_N - \boldsymbol{R}_t\boldsymbol{W}_t)^{-1}(\boldsymbol{X}_t\boldsymbol{\beta} + \boldsymbol{\varepsilon}_t) = \left(\mathbf{I}_N + \boldsymbol{R}_t\boldsymbol{W}_t + (\boldsymbol{R}_t\boldsymbol{W}_t)^2 + (\boldsymbol{R}_t\boldsymbol{W}_t)^3 + \ldots\right)(\boldsymbol{X}_t\boldsymbol{\beta} + \boldsymbol{\varepsilon}_t), \quad (12)
\end{aligned}$$

as long as the largest absolute eigenvalue of $\boldsymbol{R}_t\boldsymbol{W}_t$ is smaller than one. Apart from the composition of $\boldsymbol{R}_t$ and $\boldsymbol{W}_t$ in risk spillovers, we also want to account for the magnitude of the structural shocks as captured by the time-varying covariance matrix $\boldsymbol{\Sigma}_t$ in order to prevent increases in $\boldsymbol{R}_t$ to be off-set by decreases in $\boldsymbol{\Sigma}_t$.

We consider two risk spillover measures: a short-run (SR) and a long-run (LR) risk spillover measure, defined as

$$SR_{i,j,t} = e_i^\top \; \boldsymbol{R}_t \; \boldsymbol{W}_t \; \boldsymbol{\Sigma}_t^{1/2} \; e_j = \boldsymbol{\Sigma}_{j,j,t}^{1/2} \; \boldsymbol{R}_{i,i,t} \; \boldsymbol{W}_{i,j,t} \quad (13)$$

$$LR_{i,j,t} = e_i^\top \; (\mathbf{I}_N - \boldsymbol{R}_t \; \boldsymbol{W}_t)^{-1} \; \boldsymbol{\Sigma}_t^{1/2} \; e_j = \boldsymbol{\Sigma}_{j,j,t}^{1/2} \; (\mathbf{I}_N - \boldsymbol{R}_t \; \boldsymbol{W}_t)^{-1}_{i,j}, \quad (14)$$

respectively, with e_i $(i = 1, \ldots N)$ denoting the i-th column of $\mathbf{I}_N$. The first risk measure computes

the first-order spatial spillover effect on country i of a one standard deviation structural shock to country j. The second measure calculates the compound or reduced form effect of such a structural shock. As there are 7×7 possible combinations of countries and two risk measures, we only report a sub-selection of the results. We focus on structural shocks to 3 large Eurozone countries, namely Germany, Spain, and Italy. We provide the results for two models: scalar ρ_t and heterogeneous $\boldsymbol{R}_t$. We thus always allow for time-variation in the spatial correlations. The results are given in Figures 4 and 5 for $SR_{i,j,t}$ and $LR_{i,j,t}$, respectively.

The left-hand panels in both Figures 4 and 5 relate to the scalar model (ρ_t), whereas the right-hand panels are for the heterogeneous model ($\boldsymbol{R}_t$). In all figures, the clear decrease in volatility ($\boldsymbol{\Sigma}_{j,j,t}$) towards the end of the sample is visible for all countries considered. The decreasing standard deviations in $\boldsymbol{\Sigma}_t$ result in smaller-sized (one standard deviation) shocks to $\boldsymbol{\varepsilon}_t$. Looking at Figure 4a, we first note the effect of a one standard deviation shock to Germany in the scalar model to all other countries. Looking at the vertical axis, we see that the impacts are modest, and comparable for countries like Italy, Ireland and the Netherlands. Allowing for heterogeneous spillovers like in Figure 4b changes the picture dramatically. Particularly Italy reacts substantially to German shocks. Again, this is intuitive, Italy at the time being one of the large economies in potential distress (Romano, 2021), and Germany being the stable anchor economy. All other sensitivities are an order of magnitude smaller, with the exception of Ireland during 2011. Note that the vertical axis in Figure 4b has a much wider scale than in Figure 4a.

We see a similar effect in Figures 4c and 4d. Again note the difference in the vertical axes between the left-hand and right-hand panels. For the pooled, scalar model ρ_t the effects on all other countries are modest and comparable. If we allow for heterogeneity via $\boldsymbol{R}_t$, however, Spanish shocks mainly reflect on Portugal, which again makes intuitive sense given the close connection of these economies. Second in line are Italy and Ireland, which were also at the center of the European sovereign debt crisis. The other countries only follow at a larger distance. The dynamics of the risk spillovers based on the heterogeneous model thus follow the dynamics of the crisis much more closely than those of the homogeneous, pooled model in Figure 4c.

Also for Italy (bottom panels), the first order risk-spillover effects are different between the pooled and heterogeneous model specification, but much less so than for Germany or Spain. The most striking difference is the non-diminished spillover from Italy to France till the very end of the sample. The link to Portugal and Spain in the middle panels persists also somewhat, but much less so. We see that the spillover of Italy to France versus other countries also peaks at very different moments, again causing problems for the pooled ρ_t model to capture all these different developments well in one and the same ρ_t parameter.

Compounding the first-order spillover effects from equation (13) into their reduced from effects,

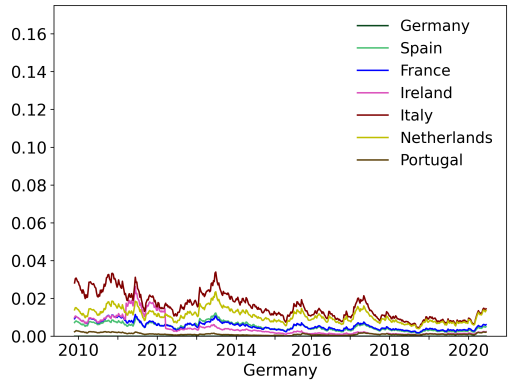

(a) German shock; ρ_t model

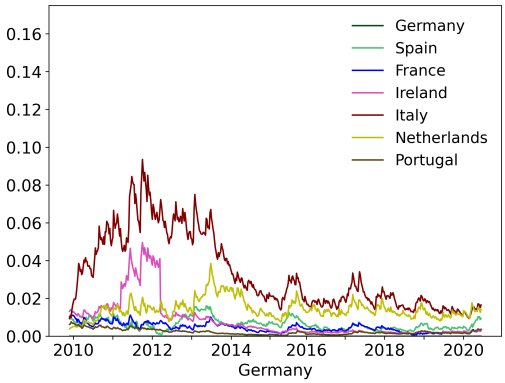

(b) German shock; $\boldsymbol{R}_t$ model

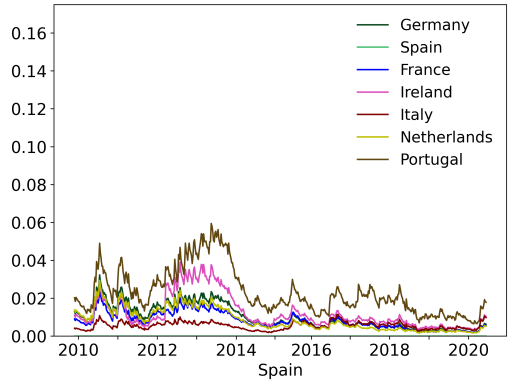

(c) Spanish shock; ρ_t model

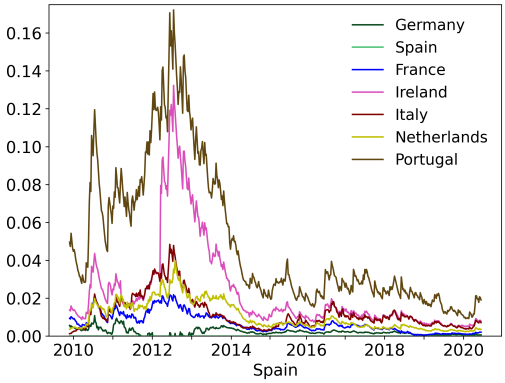

(d) Spanish shock; $\boldsymbol{R}_t$ model

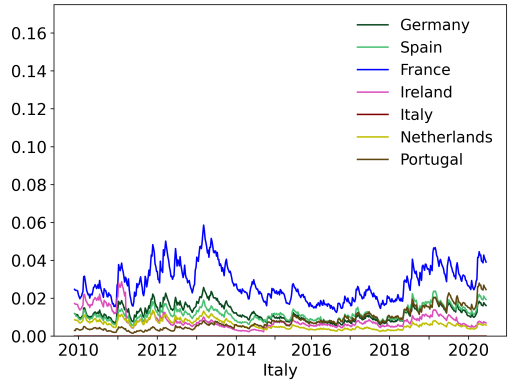

(e) Italian shock; ρ_t model

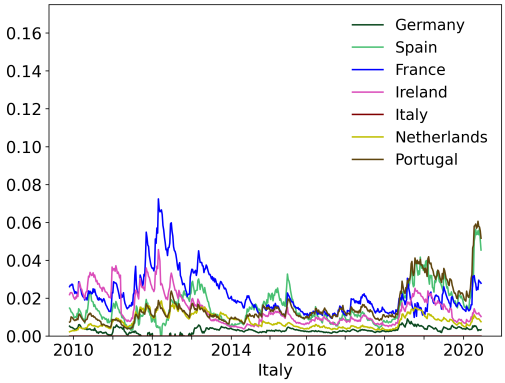

(f) Italian shock; $\boldsymbol{R}_t$ model

Figure 4: First-order spillover effects

This figure gives the first-order effect $SR_{i,j,t}$ of a 1 standard deviation shock of the government bond yield spread change of country j to country i for j equal to Germany (top panels), Spain (middle panels), or Italy (lower panels). The left-hand panels relate to the dynamic scalar spatial model. The right-hand panels correspond tot he dynamic diagonal spatial model. Spreads are denoted in basis points (bp). The sample runs from December 2009 - July 2020.

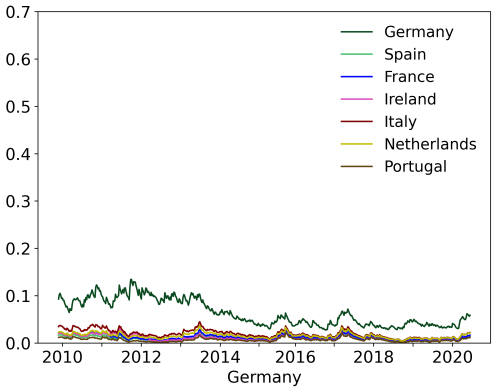

(a) German shock; ρ_t model

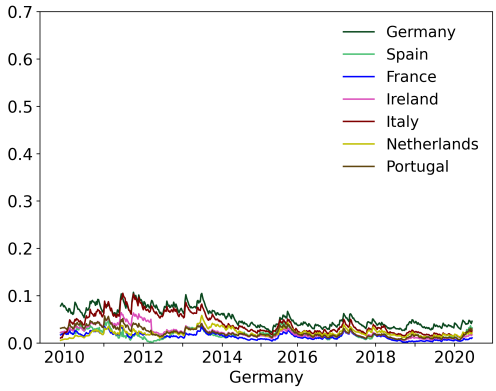

(b) German shock; $\boldsymbol{R}_t$ model

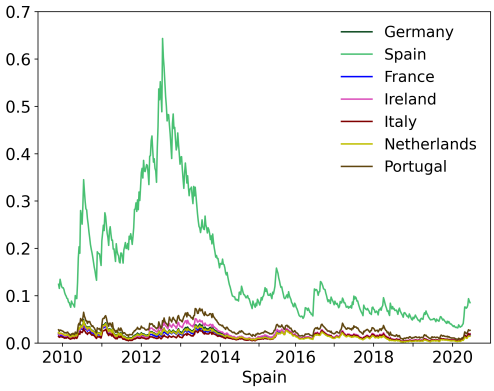

(c) Spanish shock; ρ_t model

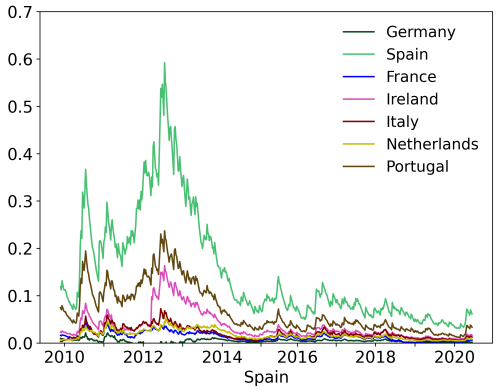

(d) Spanish shock; $\boldsymbol{R}_t$ model

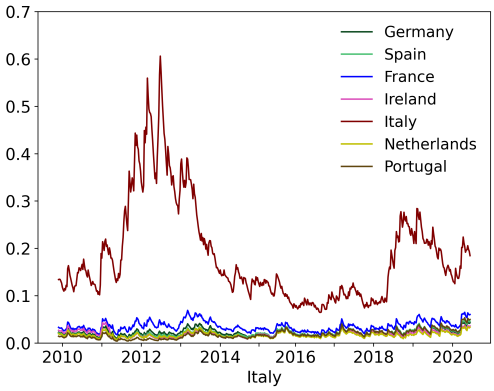

(e) Italian shock; ρ_t model

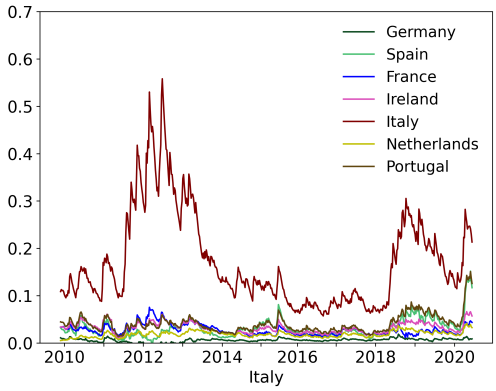

(f) Italian shock; $\boldsymbol{R}_t$ model

Figure 5: Long-term spillover effects

This figure gives the compound reduced-form effect $LR_{i,j,t}$ of a 1 standard deviation shock of the government bond yield spread of country j to country i for j equal to Germany (top panels), Spain (middle panels), or Italy (lower panels). The left-hand panels relate to the dynamic scalar spatial model. The right-hand panels correspond tot he dynamic diagonal spatial model. The sample runs from December 2009 - July 2020.

we obtain the patterns in Figure 5. Again, we see a number of striking differences between the standard scalar models versus the heterogeneous models. For the scalar models, a one standard deviation shock only appears to have a sizeable reduced form effect on the country itself. This holds for all countries considered, the effect in basis points (vertical axes) being understandably higher for Spain and Italy than for Germany.

The most interesting patterns can be seen in the right-hand plots in Figure 5. One-standard-deviation shocks to Germany in Figure 5a result in a maximum effect of around 0.14bp on Germany and 0.04bp on Italy. In Figure 5b, however, we see that though the effect of Germany on Germany itself remains the largest for the heterogeneous model, with a few exceptions, it is now closely followed by the effect on Italy with about 0.1bp. Also Spain, Ireland, and Portugal have a much higher dependence on Germany in the heterogeneous model. This confirms Germany's role as an anchor of the Eurozone, a feature that would have been fully unclear in the standard pooled spatial model.

We see a similar intuitive effect for Spanish shocks in Figure 5d. The heterogeneous model has the largest effect on Spain itself with a maximum of around 0.6bp. It is followed by the effect on Portugal. This reduced-form spillover was not apparent for the homogeneous model from Figure 5c. For example, whereas the scalar spatial model leads from a one standard deviation shock to Spain to a reduced-form increase to Portugal of only 0.05 bp in July 2012, according to the diagonal spatial model this effect increases by more than a factor 5 to 0.25 bp.

Finally, for Italy the reduced form effect of an Italian structural shock is largest on Italy, and quite comparable between the scalar ρ_t and heterogeneous $\boldsymbol{R}_t$ model. The effects on other countries are around zero throughout till the end of sample mid 2020 (start of the covid crisis), with the exception of Spain and Portugal peaking at the beginning of 2020, particularly for the heterogeneous model.

We conclude that allowing for heterogeneous, time-varying spatial correlations has a prominent and empirically relevant effect on measuring risk spillover across Europe. The empirical features that emerge are more intuitive and cannot be recovered by models without either time-variation or heterogeneity. We expect such effects to be potentially similarly important for other dynamic networks. Also in those settings, standard static or dynamic network models based on pooled spatial spillovers may be much to restrictive to uncover the real network dynamics and dominant risk players in the network. Models of the form presented in the current paper are likely to fare considerably better in this respect and be empirically more accurate. Given that the current models are still straightforward to estimate, such additional flexibility comes at little to no computational cost.

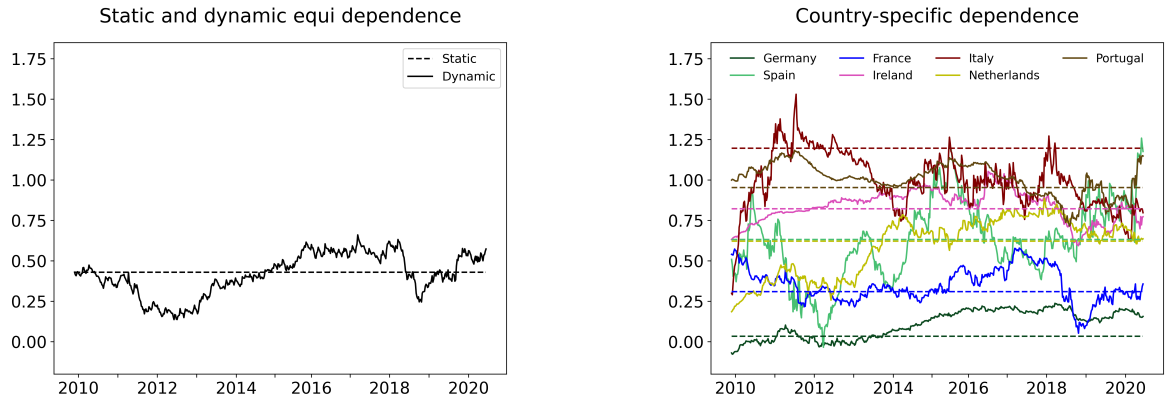

(a) (b)

Figure 6: Filtered spatial autoregressive parameters after U.S. correction

This figure depicts fitted dependencies from four different models, applied to changes of government bond yield spreads of seven European countries after taking out the effect of U.S. yield spread changes over EONIA. The left figure depicts the fixed and time-varying equi-spatial dependencies, whereas the right figure shows the heterogeneous and time-varying dependencies through time. The sample runs from December 2009 - July 2020.

5 Robustness checks

In this section, we first show that our main results persist if we correct European yield changes for U.S. yield changes as a possibly omitted common factor. Second, we show that are results do not hinge of the use of the 5 govenment bond year yields. Also for 1 year bond yields as well as for 5 year CDS spreads, allowing for heterogeneity as well as time-variation in the spatial network model proves important. In all robustness analysis, we keep the observed matrix $\boldsymbol{W}_t$ the same as in the baseline analysis.

5.1 Remove common global (U.S.) factor

In spatial regression models, there is a concern (Hale and Lopez, 2019) that the network effects may in part be confounded with a missing common factor. In our current context of spillover effects in Eurozone countries, network effects could mix in with an omitted global common government credit risk factor. As a robustness check, we therefore introduce the U.S. government bond yield spread as an observed common factor. In a first step, we regress all Eurozone yield changes on the U.S. yield changes to take out the common factor. Subsequently, we redo our analysis using the residuals of these regressions as our dependent variables.

Figure 6 reports the new filtered heterogeneous spatial dependence parameters. It is clear that the spatial spillover strength across government yield changes remains remarkably heterogeneous.

Table 3: Log-likelihood AIC values for models based on 1-year government bond yield spreads and 5 year CDS spread data.
Set-up is similar as in Table 2.

	Static Scalar	Dynamic Scalar	Static Diagonal	Dynamic Diagonal
Panel A: 1y bond yields over EONIA				
logLik	4733	4764	4778	4811
AIC	-9424	-9482	-9503	-9551
Panel B: 5y Euro denominated CDS				
logLik	-10562	-10540	-10284	-10225
AIC	21167	21126	20622	20520

Countries like Italy, Spain, and Portugal still exhibit high spatial dependence strength during the crisis, whereas a country like Germany has low and somtimes even negative spatial dependence. Though some of the patterns change slightly when first taking out the common U.S. component, the overall picture in Figure 6 remains remarkably similar compared to that in Figure 3.

5.2 The alternative dependent variables

As a second robustness check, we confirm that the importance of time-variation and heterogeneity in dynamic networks for the Eurozone is not confined to the use of 5 year government bond yields. In paricular, we analyze Euro denominated 5-year CDS (credit default swap) spread changes as well as changes in 1-year government yields over the 1-year EONIA OIS rate. This provides two alternative data sets. The relevant data are retrieved from Datastream and Bloomberg. The summary statistics of these data are provided in the appendix. Like the 5-year bond yield changes, both the 1-year yields and the 5-year CDS rates exhibit clear signs of fat-tailedness and outliers, such that our use of the fat-tailed Student t distribution and the time-variation in $\boldsymbol{\Sigma}_t$ seem warranted.

Table 3 and Figure 7 summarize the main results. Full estimation results including all parameters and standard errors are provided in the appendix. The likelihood and AIC values in Table 3 For the 1-year spreads, we confirm the value-added of both the heterogeneity (plus 45 likelihood points) and the time-variation (plus another 33 likelihood points) A similar result holds for the 5 year CDS spreads, with an increase of 278 likelihood points for adding heterogeneity, and a further 59 points for the time variation. In both cases, the AIC values are clearly lowest for the heterogeneous network model with time-varying parameters.

Figure 7 shows the pictures of the fitted ρ_t and $\boldsymbol{R}_{i,i,t}$s. As in our baseline analysis, we see that the magnitude as well as the dynamics of the scalar ρ_t are heavily limited due to the heterogeneity and time-variation in the data. Because of all this pooling, hardly any interesting signal is left in the scalar ρ_t. By contrast, for instance for the 1 year results, we again see the dominance in spatial

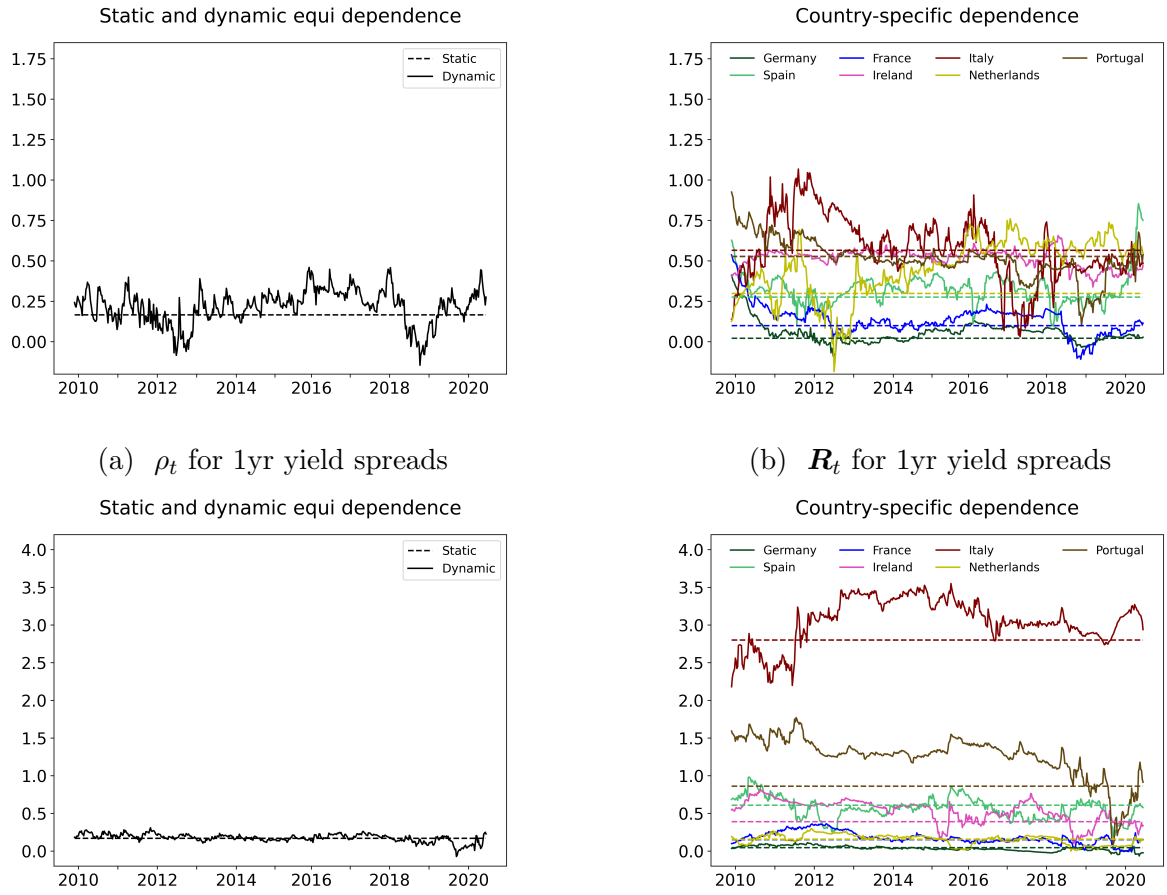

(a) ρ_t for 1yr yield spreads

(b) $\boldsymbol{R}_t$ for 1yr yield spreads

(c) ρ_t for 5 yr CDS spreads

(d) $\boldsymbol{R}_t$ for 5 yr CDS spreads

Figure 7: Filtered spatial autoregressive parameters for 1-year bond yield EONIA spread changes and 5 year CDS spread changes

This figure depicts fitted dependencies from four different models, applied to changes of government bond yield spreads of seven European countries after taking out the effect of U.S. yield spread changes over EONIA. The left figure depicts the fixed and time-varying equi-spatial dependencies, whereas the right figure shows the heterogeneous and time-varying dependencies through time. The sample runs from December 2009 - July 2020.

sensitivity of countries like Italy and Portugal, the opposite movements of Italy versus most other countries during the first years of the sample (i.e., the sovereign debt crisis), and the sudden rise of Spain during the start of the covid pandemic.

The results for the CDS rates are also interesting. These markets do not behave in full lock-step with the bond markets over the sample period. Still, the importance of both network dynamics and network heterogeneity are evident from the picture. The pooled, scalar ρ_t hardly shows any time variation except towards the end of the sample. Note that the level of ρ_t for the 5 year CDS spreads is almost the same as for the 1 year bond yield spreads. The cross-sectional variation in $\boldsymbol{R}_{i,i,t}$ for the CDS spreads is even larger than for bond spreads. Again, Italy and Portugal

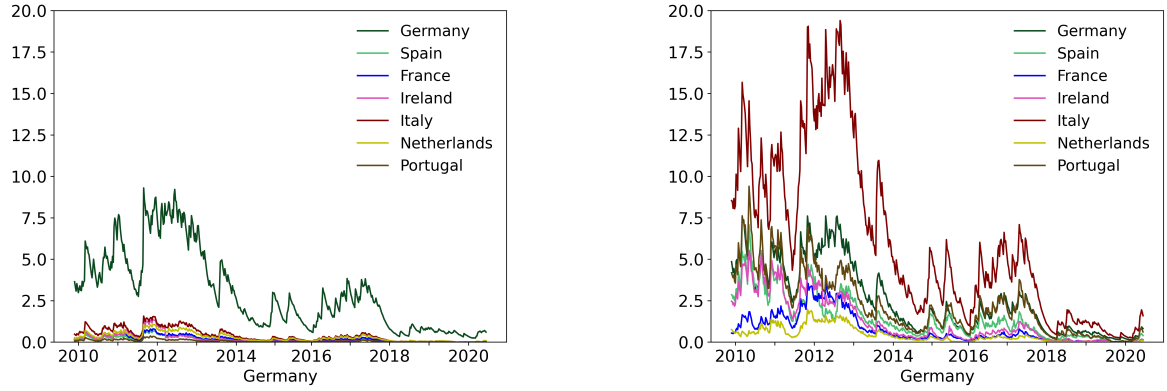

(a) (b)

Figure 8: compound reduced-form risk spillover effect $LR_{i,j,t}$ for a one-standard deviation German shock based on 5-year CDS spread data

This figure gives the compound reduced-form effect $LR_{i,j,t}$ of a 1 standard deviation shock of the government bond yield spread of Germany to other Eurozone countries based on models estimated with 5 year CDS spread changes as the dependent variable. The left-hand panels relate to the dynamic scalar spatial model. The right-hand panels correspond tot he dynamic diagonal spatial model. The sample runs from December 2009 - July 2020.

are clearly at the top, followed by Spain and Ireland. The size of $\boldsymbol{R}_{i,i,t}$ is substantially above 1 for both Italy and Portugal, without jeopardizing the stability of the model, i.e., $\boldsymbol{R}_t\boldsymbol{W}_t$ still has all eigenvalues inside the unit circle at all times. Also the CDS data show the importance of heterogeneity in time-variation: we also confirm for this data the different, increasing pattern in $\boldsymbol{R}_{i,i,t}$ for Italy during the first years of the sample, whereas countries like Spain and Portugal show a downward trend during that same period. As a result, hardly any pattern is left in the scalar ρ_t. Pooling of all these parameters is therefore not a good idea for obtaining a clear picture of what is happening in the data, and the proposed dynamic heterogeneous spatial model provides a good alternative.

Finally, Figure 8 shows a prototypical picture of the effect on risk measures based on these alternative datasets. We concentrate on the CDS spread data models and the total, reduced form risk spillover $LR_{i,j,t}$ of a one standard deviation shock to Germany on the other Eurozone countries. We see a similar effect as in Figure 5. In the scalar model, the effect of a German shock mainly affects Germany after all spillovers have been taken into account. However, if we allow for heterogeneity, the picture changes dramatically. Particularly during the sovereign debt crisis, German shocks also heavily affect Spain, Portugal, Ireland, and particularly Italy. This is fully in line with the story of the European sovereign debt crises, and not recovered by the simpler, pooled standard models.

6 Conclusion

In this paper, we proposed a new model for dynamic risk networks with heterogeneous and dynamic spatial dependence coefficients. We proved that such models are much more effective in describing dynamic risk networks than standard, homogeneous static spatial models. Discarding heterogeneity or time-variation of the network connections can lead to flawed conclusions about the major players in the network and their position over time. By contrast, the new model was successful in uncovering such patterns. Though flexible, the model remains tractable and straightforward to estimate using maximum likelihood methods.

We applied the new model to three different datasets related to Europe perceived sovereign credit risk over the period 2009-2020. Using pooled spatial dynamics as in standard network models appeared quite disastrous for uncovering the importance of the different players over time. In particular, the anchoring role of Germany for the Eurozone only becomes clear if sufficient heterogeneity is allowed for. Similarly, risk connectedness of players like Spain, Portugal, and Italy only emerged upon allowing for heterogeneity as well as time-variation, irrespective of which of the three datasets was used. Empirical models for network dynamics should thus carefully account for such differences in spillover strength and their time-variation if they are to help the researcher finding the true story in the data and the correct assessment of risk.

References

Acemoglu, D., A. Ozdaglar, and A. Tahbaz-Salehi (2015). Systemic risk and stability in financial networks. *American Economic Review 105*(2), 564–608.

Acharya, V., I. Drechsler, and P. Schnabl (2014). A pyrrhic victory? bank bailouts and sovereign credit risk. *The Journal of Finance 69*(6), 2689–2739.

Anselin, L. (2009). Spatial regression. *The SAGE handbook of spatial analysis 1*, 255–276.

Aquaro, M., N. Bailey, and M. H. Pesaran (2021). Estimation and inference for spatial models with heterogeneous coefficients: an application to us house prices. *Journal of Applied Econometrics 36*(1), 18–44.

Asgharian, H., W. Hess, and L. Liu (2013). A spatial analysis of international stock market linkages. *Journal of Banking & Finance 37*(12), 4738–4754.

Babii, A., X. Chen, and E. Ghysels (2019). Commercial and residential mortgage defaults: Spatial dependence with frailty. *Journal of Econometrics 212*(1), 47–77.

Billé, A. G., F. Blasques, and L. Catania (2019). Dynamic spatial autoregressive models with time-varying spatial weighting matrices. *Available at SSRN 3241470*.

Billio, M., M. Getmansky, A. W. Lo, and L. Pelizzon (2012). Econometric measures of connectedness and systemic risk in the finance and insurance sectors. *Journal of financial economics 104*(3), 535–559.

Blasques, F., S. J. Koopman, and A. Lucas (2015). Information-theoretic optimality of observation-driven time series models for continuous responses. *Biometrika 102*(2), 325–343.

Blasques, F., S. J. Koopman, A. Lucas, and J. Schaumburg (2016). Spillover dynamics for systemic risk measurement using spatial financial time series models. *Journal of Econometrics 195*(2), 211–223.

Blasques, F., J. van Brummelen, S. Koopman, and A. Lucas (2021). Maximum likelihood estimation for generalized autoregressive score models. *Journal of Econometrics*, in press.

Catania, L. and A. G. Billé (2017). Dynamic spatial autoregressive models with autoregressive and heteroskedastic disturbances. *Journal of Applied Econometrics 32*(6), 1178–1196.

Creal, D., S. J. Koopman, and A. Lucas (2011). A dynamic multivariate heavy-tailed model for time-varying volatilities and correlations. *Journal of Business & Economic Statistics 29*(4), 552–563.

Creal, D., S. J. Koopman, and A. Lucas (2013). Generalized autoregressive score models with applications. *Journal of Applied Econometrics 28*(5), 777–795.

Creal, D., S. J. Koopman, A. Lucas, and M. Zamojski (2020). Generalized autoregressive method of moments.

Demirer, R., R. Ferrer, and S. J. H. Shahzad (2020). Oil price shocks, global financial markets and their connectedness. *Energy Economics 88*, 104771.

Denbee, E., C. Julliard, Y. Li, and K. Yuan (2021). Network risk and key players: A structural analysis of interbank liquidity. *Journal of Financial Economics 141*, 831–859.

Diebold, F. X. and K. Yılmaz (2014). On the network topology of variance decompositions: Measuring the connectedness of financial firms. *Journal of Econometrics 182*(1), 119–134.

Elliott, M., B. Golub, and M. O. Jackson (2014). Financial networks and contagion. *American Economic Review 104*(10), 3115–53.

Fernandes, G. B. and R. Artes (2016). Spatial dependence in credit risk and its improvement in credit scoring. *European Journal of Operational Research 249*(2), 517–524.

Fernandez, V. (2011). Spatial linkages in international financial markets. *Quantitative Finance 11*(2), 237–245.

Fernández-Avilés, G., J.-M. Montero, and A. G. Orlov (2012). Spatial modeling of stock market comovements. *Finance Research Letters 9*(4), 202–212.

Franklin, A. and G. Douglas (2000). financial contagion. *Journal of Political Economy 108*(1), 1–33.

Hale, G. and J. A. Lopez (2019). Monitoring banking system connectedness with big data. *Journal of Econometrics 212*(1), 203–220.

Harvey, A. and A. Luati (2014). Filtering with heavy tails. *Journal of the American Statistical Association 109*(507), 1112–1122.

Harvey, A. C. (2013). *Dynamic models for volatility and heavy tails: with applications to financial and economic time series*, Volume 52. Cambridge University Press.

Herskovic, B., B. Kelly, H. Lustig, and S. Van Nieuwerburgh (2020). Firm volatility in granular networks. *Journal of Political Economy 128*(11), 4097–4162.

Kou, S., X. Peng, and H. Zhong (2018). Asset pricing with spatial interaction. *Management Science 64*(5), 2083–2101.

Milcheva, S. and B. Zhu (2016). Bank integration and co-movements across housing markets. *Journal of Banking & Finance 72*, S148–S171.

Pino, G. and S. C. Sharma (2019). On the contagion effect in the us banking sector. *Journal of Money, Credit and Banking 51*(1), 261–280.

Romano, S. (2021). The 2011 crisis in italy: A story of deep-rooted (and still unresolved) economic and political weaknesses. In *Financial Crisis Management and Democracy*, pp. 173–184. Springer, Cham.

Tonzer, L. (2015). Cross-border interbank networks, banking risk and contagion. *Journal of Financial Stability 18*, 19–32.

Williamson, S. D. (2003). Payments systems and monetary policy. *Journal of Monetary Economics 50*(2), 475–495.

Zhu, B. and C. Lizieri (2021). Connected markets through global real estate investments. *Real Estate Economics 49*, 618–654.

Zhu, B. and S. Milcheva (2020). The pricing of spatial linkages in companies' underlying assets. *The Journal of Real Estate Finance and Economics 61*(3), 443–475.

Appendix to: The Importance of Heterogeneity in Dynamic Network Models Applied to European Systemic Risk

Xingmin Zhang[a], Anne Opschoor[b], and André Lucas[b]

[a] *School of Finance, Southwestern University of Finance and Economics, China*

[b] *Vrije Universiteit Amsterdam and Tinbergen Institute*

A Score-driven time-varying parameters

The score updates in our model drive the two diagonal time-varying matrices $\boldsymbol{R}_t = \boldsymbol{R}(\boldsymbol{f}_t)$ and $\boldsymbol{\Sigma}_t = \boldsymbol{\Sigma}(\boldsymbol{f}_t)$, where we gathered the time-varying parameters in a vector $\boldsymbol{f}_t$ as in equation (2). The log predictive density is given by

$$\begin{aligned}\log p_{\boldsymbol{y}}\left(\boldsymbol{y}_t; \boldsymbol{R}(\boldsymbol{f}_t), \boldsymbol{\Sigma}(\boldsymbol{f}_t), \nu\right) &= \log\Gamma\left(\frac{\nu+N}{2}\right) - \log\Gamma\left(\frac{\nu}{2}\right) - \frac{N}{2}\log\left(\nu-2\right) - \frac{N}{2}\log\left(\pi\right) \\ &- \frac{1}{2}\log\mid\boldsymbol{\Sigma}_t\mid + \log\mid\mathbf{I}_N - \boldsymbol{R}_t\boldsymbol{W}_t\mid - \frac{\nu+N}{2}\log\left(1+\frac{\boldsymbol{e}_t^\top\boldsymbol{\Sigma}_t^{-1}\boldsymbol{e}_t}{(\nu-2)}\right), \end{aligned} \tag{A.1}$$

with $\boldsymbol{e}_t$ defined as in (8). For $\boldsymbol{R}_{i,i,t} = h\left(f_{i,t}\right) = f_{i,t}$ for $i = 1, \ldots, N$, we obtain the unit scaled score

$$\boldsymbol{s}_{i,t} = \left(\frac{\partial \log p_{\boldsymbol{y}}\left(\boldsymbol{y}_t; \boldsymbol{R}_t, \boldsymbol{\Sigma}_t, \nu\right)}{\partial \boldsymbol{R}_{i,i,t}}\right)\left(\frac{\partial h\left(f_{i,t}\right)}{\partial f_{i,t}}\right) = \frac{\partial \log p_{\boldsymbol{y}}\left(\boldsymbol{y}_t; \boldsymbol{R}_t; \boldsymbol{\Sigma}_t, \nu\right)}{\partial \boldsymbol{R}_{i,i,t}}.$$

For other parameterizations of $\boldsymbol{R}_{i,i,t}$ as a function of $\boldsymbol{f}_t$, the second factor does not drop from the equation. Let $\boldsymbol{E}_i$ be an $N \times N$ matrix of zeros, with a a single 1 on the ith diagonal element.[5] Using the density expression in (A.1) and the definition of w_t and $\boldsymbol{y}_t^\star$ in (9) and (7), respectively,

[5] Again, for different parameterizations of $\boldsymbol{R}_{i,i,t}$, $\boldsymbol{E}_i$ in the below derivations for $\boldsymbol{R}_{i,i,t}$ (though not for $\boldsymbol{\Sigma}_{i,i,t}$) has to be replaced by $\boldsymbol{E}_i \cdot \partial h(f_{i,t})/\partial f_{i,t}$.

we obtain

$$\begin{aligned}
\boldsymbol{s}_{i,t} &= w_t\ \boldsymbol{e}_t^\top \boldsymbol{\Sigma}_t^{-1} \frac{\partial \boldsymbol{R}_t}{\partial f_{i,t}} \boldsymbol{W}_t \boldsymbol{y}_t - \operatorname{vec}\left(\left((\mathbf{I}_N - \boldsymbol{R}_t \boldsymbol{W}_t)^{-1}\right)^\top\right) \operatorname{vec}\left(\frac{\partial \boldsymbol{R}_t}{\partial f_{i,t}} \boldsymbol{W}_t\right) \\
&= w_t\ \boldsymbol{e}_t^\top \boldsymbol{\Sigma}_t^{-1} \boldsymbol{E}_i \boldsymbol{y}_t^\star - \operatorname{vec}\left(\left((\mathbf{I}_N - \boldsymbol{R}_t \boldsymbol{W}_t)^{-1}\right)^\top\right) \operatorname{vec}\left(\boldsymbol{E}_i \boldsymbol{W}_t\right) \\
&= w_t\ \boldsymbol{e}_{i,t}^\top \boldsymbol{\Sigma}_{i,i,t}^{-1} \boldsymbol{y}_{i,t}^\star - \operatorname{trace}\left((\mathbf{I}_N - \boldsymbol{R}_t \boldsymbol{W}_t)^{-1} \boldsymbol{E}_i \boldsymbol{W}_t\right) \\
&= w_t\ \boldsymbol{e}_{i,t}^\top \boldsymbol{\Sigma}_{i,i,t}^{-1} \boldsymbol{y}_{i,t}^\star - \left(\boldsymbol{W}_t \left(\mathbf{I}_N - \boldsymbol{R}_t \boldsymbol{W}_t\right)^{-1}\right)_{i,i}
\end{aligned}$$

for $i = 1, \ldots, N$. For $\nu \to +\infty$, we see $w_t \to 1$ and the score function vector collapses to that of multivariate normal distribution.

For the scores with respect to $f_{i+N,t} = \log \boldsymbol{\Sigma}_{i,i,t}$, using the diagonality of $\boldsymbol{\Sigma}_t$, we have

$$\begin{aligned}
\boldsymbol{s}_{i+N,t} &= \frac{\partial \log p_{\boldsymbol{y}}\left(\boldsymbol{y}_t; \boldsymbol{R}(\boldsymbol{f}_t), \boldsymbol{\Sigma}(\boldsymbol{f}_t), \nu\right)}{\partial f_{i+N,t}} = \frac{\partial \log p_{\boldsymbol{y}}\left(\boldsymbol{y}_t; \boldsymbol{R}_t, \boldsymbol{\Sigma}_t, \nu\right)}{\partial \boldsymbol{\Sigma}_{i,i,t}} \frac{\partial \exp\left(f_{i+N,t}\right)}{\partial f_{i+N,t}} \\
&= \left(-\frac{1}{2\boldsymbol{\Sigma}_{i,i,t}} + \tfrac{1}{2} w_t\ \frac{\boldsymbol{e}_{i,t}^2}{\boldsymbol{\Sigma}_{i,i,t}^2}\right) \cdot \exp\left(f_{i+N,t}\right) = \left(-\frac{1}{2\boldsymbol{\Sigma}_{i,i,t}} + \tfrac{1}{2} w_t\ \frac{\boldsymbol{e}_{i,t}^2}{\boldsymbol{\Sigma}_{i,i,t}^2}\right) \cdot \boldsymbol{\Sigma}_{i,i,t} \\
&= \tfrac{1}{2} w_t\ \frac{\boldsymbol{e}_{i,t}^2}{\boldsymbol{\Sigma}_{i,i,t}} - \frac{1}{2}.
\end{aligned}$$

B Extra empirical results

This appendix presents additional empirical results for 1-year government bond yield spread changes (over EONIA) and for 5-year CDS spread changes.

Table B.1: Summary statistics 1-year Government Yield spread and CDS spreads

This table lists descriptive statistics of absolute changes of Euro-denominated CDS spreads and 1-year government yield spreads of seven European countries and the United States. The 1-year yield spread is defined as the difference between the 1-year government bond yield and the 1-year EONIA OIS rate. All variables are weekly from December 10, 2009 until July 2, 2020.

	mean	s.d.	med	min	max	skew	kurt
1-year gov bond spread changes (percentage points)							
Germany	-0.001	0.041	0.001	-0.19	0.21	-0.21	6.83
Spain	0.001	0.228	-0.001	-1.27	2.86	3.45	52.46
France	-0.001	0.057	0.001	-0.59	0.45	-0.91	32.73
Ireland	-0.001	0.397	-0.001	-2.73	3.42	0.01	29.41
Italy	0.000	0.228	-0.002	-1.02	1.36	0.86	12.07
Netherland	0.000	0.060	0.000	-0.54	0.64	0.16	45.60
Portugal	-0.001	0.553	-0.002	-3.12	2.78	-0.19	14.11
U.S.	0.002	0.062	0.006	-0.56	0.25	-1.71	17.04
5-year CDS spread changes (basis points)							
Germany	-0.025	2.867	0.000	-19.02	15.19	0.09	14.05
Spain	-0.036	17.570	-0.080	-109.51	87.30	-0.56	12.61
France	-0.028	6.382	0.000	-54.84	37.90	-0.84	20.69
Ireland	-0.231	24.841	-0.200	-154.33	223.13	0.83	25.33
Italy	0.051	19.320	-0.400	-99.03	98.74	-0.29	11.33
Netherland	-0.033	4.861	0.000	-42.02	28.31	-1.95	32.72
Portugal	-0.042	39.428	-0.050	-255.23	252.21	0.30	15.53
U.S.	-0.026	2.237	0.000	-12.81	16.76	1.24	17.70

Table B.2: Parameter estimates of spatial dependence models 1-year government bond yield spreads

This table reports the estimated parameters of four spatial dependence models, applied to weekly 1 year government bond yield spread changes of seven Eurozone countries. Robust (Huber sandwich) standard errors are reported in parentheses. The models are based on Student's t distributed disturbances with time-varying heteroscedasticity as in model (1)–(4). We report the maximum log-likelihood value (LogLike) and AIC(Akaike information criterion). The sample runs from December 2009 - July 2020.

	Static Scalar	Dynamic Scalar	Static Diagonal	Dynamic Diagonal
Panel A: Spatial dependence parameters				
ω/ω_{GE}	0.167	0.020	0.022	0.000
	(0.026)	(0.010)	(0.030)	(0.001)
ω_{SP}			0.276	0.010
			(0.055)	(0.009)
ω_{FR}			0.099	0.003
			(0.035)	(0.004)
ω_{IR}			0.529	0.015
			(0.107)	(0.015)
ω_{IT}			0.566	0.035
			(0.171)	(0.029)
ω_{NE}			0.299	0.015
			(0.058)	(0.014)
ω_{PO}			0.528	0.015
			(0.157)	(0.020)
α/α_{GE}		0.011		0.005
		(0.002)		(0.008)
α_{SP}				0.021
				(0.021)
α_{FR}				0.007
				(0.002)
α_{IR}				0.033
				(0.082)
α_{IT}				0.170
				(0.089)
α_{NE}				0.027
				(0.016)
α_{PO}				0.053
				(0.077)
β_ρ		0.919		0.974
		(0.046)		(0.027)

(Table B.2 continued)

	Static Scalar	Dynamic Scalar	Static Diagonal	Dynamic Diagonal
Panel B: Volatility and control parameters				
α_{vol}	0.334	0.328	0.328	0.322
	(0.047)	(0.039)	(0.041)	(0.032)
β_{vol}	0.996	0.997	0.996	0.997
	(0.004)	(0.004)	(0.004)	(0.002)
ν	3.374	3.354	3.517	3.491
	(0.275)	(0.273)	(0.293)	(0.287)
Δ VSTOXX	-0.015	-0.016	-0.019	-0.014
	(0.039)	(0.036)	(0.038)	(0.035)
Δ term spread	-0.050	-0.047	-0.057	-0.042
	(0.047)	(0.044)	(0.047)	(0.045)
local stock	-0.001	0.001	0.000	0.001
	(0.010)	(0.009)	(0.009)	(0.009)
logLik	4733	4764	4778	4811
AIC	-9424	-9482	-9503	-9551

Table B.3: Parameter estimates of spatial dependence models

This table reports the estimated parameters of four spatial dependence models, applied to weekly CDS spread changes of seven Eurozone countries. Robust (Huber sandwich) standard errors are reported in parentheses. The models are based on Student's t distributed disturbances with time-varying heteroscedasticity as in model (1)–(4). To account for the different measurement units of the CDS changes (basis points) compared to the yield spread changes in the other tables, the VSTOXX change was rescaled by a factor 100. We report the maximum log-likelihood value (LogLike) and AIC(Akaike information criterion). The sample runs from December 2009 - July 2020.

	Static Scalar	Dynamic Scalar	Static Diagonal	Dynamic Diagonal
Panel A: Spatial dependence parameters				
ω/ω_{GE}	0.170	0.014	0.045	-0.001
	(0.014)	(0.011)	(0.020)	(0.001)
ω_{SP}			0.609	0.005
			(0.055)	(0.009)
ω_{FR}			0.153	0.001
			(0.023)	(0.003)
ω_{IR}			0.391	0.007
			(0.037)	(0.008)
ω_{IT}			2.802	0.187
			(0.277)	(0.089)
ω_{NE}			0.156	0.002
			(0.026)	(0.003)
ω_{PO}			0.861	0.026
			(0.109)	(0.030)
α/α_{GE}		0.003		0.001
		(0.002)		(0.001)
α_{SP}				0.026
				(0.022)
α_{FR}				0.004
				(0.002)
α_{IR}				0.020
				(0.009)
α_{IT}				0.181
				(0.083)
α_{NE}				0.005
				(0.020)
α_{PO}				0.052
				(0.061)
β_{ρ}		0.923		0.987
		(0.059)		(0.013)

(Table B.3 continued)

	Static Scalar	Dynamic Scalar	Static Diagonal	Dynamic Diagonal
Panel B: Volatility and control parameters				
α_{vol}	0.344	0.338	0.350	0.339
	(0.033)	(0.034)	(0.036)	(0.038)
β_{vol}	0.999	0.999	0.999	0.999
	(0.000)	(0.000)	(0.001)	(0.001)
ν	2.537	2.512	2.780	2.859
	(0.249)	(0.246)	(0.313)	(0.332)
Δ VSTOXX	-0.780	-0.973	-0.377	-0.323
	(0.570)	(0.596)	(0.953)	(0.899)
local gov spread	-2.648	-2.857	-2.573	-2.221
	(1.134)	(1.079)	(1.843)	(1.587)
local stock	-0.111	-0.075	-0.226	-0.167
	(0.270)	(0.231)	(0.252)	(0.327)
logLik	-10562	-10540	-10284	-10225
AIC	21167	21126	20622	20520